Tesi di Dottorato di GIULIA SCALCIONE
Matricola 784957

***POLITECNICO DI MILANO***

DIPARTIMENTO
DI
CHIMICA,
**MATERIALI**
**E**
**INGEGNERIA CHIMICA**
**"Giulio Natta"**

# CYCLOOLEFIN COPOLYMERS WITH NEW TRANSITION METAL CATALYSTS

**Dottorato di Ricerca in**
**Chimica Industriale e**
**Ingegneria Chimica (CII)**

XXVII ciclo

Coordinatore: prof. Faravelli Tiziano
Tutore: prof. Resnati Giuseppe
Relatore: dott. Incoronata Tritto

# Lista delle pubblicazioni

1. Ravasio A, Boggioni L, Scalcione G, Bertini F, Piovani D, Tritto I "Living Copolymerization of Ethylene with Norbornene by Fluorinated Enolatoimine Titanium Catalyst", *Journal of Polymer Science part A: Polymer Chemistry,* 50, *18,* pp. 3867-3874 (2012).

2. Tritto I, Boggioni L, Ravasio A, Scalcione G "Cycloolefins copolymers by Early and Late Transition Metal Catalysts", *Macromolecular Reaction Engineering*, 7, *2,* pp. 91-97 (2013).

3. Boccia AC, Scalcione G, Boggioni L, Tritto I "Multinuclear NMR Spectroscopic Characterization of a Fluorinated Enolatoimino Titanium Catalyst for the Living Ethylene-*co*-Norbornene Polymerization", *Organometallics*, 33, *10*, pp. 2510-2516 (2014).

# Sommario

# Indice delle figure

**Chapter 1: Introduction**

**Chapter 2: Copolymers and block copolymers synthesis**



**Chapter 3: Multinuclear NMR analysis for the active species**

# Indice degli schemi

# Indice delle tabelle

# Abstract

Complex [Ti($\kappa^2$-N,O-{2,6-$F_2C_6H_3N$=C(Me)C(H)=C($CF_3$)O})$_2Cl_2$] (**1**) was evaluated as catalyst for living copolymerization of ethylene (E) with norbornene (N) upon activation with dried methylaluminoxane (*d*-MAO) at temperatures between 25 and 90 °C. Copolymerization performed at different [N]/[E] feed ratios afforded stereoirregular alternating high molar mass P(E-*co*-N) with narrow molar mass distribution. The living nature of E-*co*-N copolymerization by **1**/*d*-MAO was demonstrated by kinetics at 50 °C. This catalyst system was used for the synthesis of block copolymers such as polyethylene (PE)-*block*-P(E-*co*-N) with a crystalline PE block and an amorphous P(E-*co*-N) block as well as P(E-*co*-N)$_1$-*block*-P(E-*co*-N)$_2$, having different norbornene contents in the segments and thus having different $T_g$ values.

Moreover, a multinuclear NMR spectroscopic study was performed to assess the nature of species responsible for living E-N copolymerization reaction using the catalytic system **1**/*d*-MAO. The analysis involved (i) the catalytic system (1 with MAO); (ii) the species formed after simultaneous addition of $^{13}$C-enriched ethylene and norbornene and after further addition of $^{13}$C-enriched ethylene; and (iii) species formed during norbornene homopolymerization. The results supported the existence of noncovalent interactions of *ortho*-fluoroaryl substituents with the titanium center, which contribute to the living character of the copolymerization reaction.

# 1 Introduction

## 1.1 Introduction

Polymeric materials are fundamental to our life, and their production has passed from 1.7 Mt $a^{-1}$ in 1950 to 288 Mt $a^{-1}$ in 2012 [1], since the discovery of Ziegler and Natta. Based on annual production volume, polyolefins are by far the most important commercial class of synthetic polymers. They are used on a vast scale as food packaging, coatings, building materials or household items. Moreover, technological improvements have been achieved by further developing already established processes and applying cheap monomers in new processes. In other words, the real course of development has not led to a replacement of cheap, low-value and well known materials by more expensive, more valuable ones, but rather to a specialization by developing and improving the cheapest possible polymer materials, the polyolefins.

Precise control over product structure is the goal of all chemical synthesis. In particular in the field of polymer synthesis, the structure of the resultant macromolecule is intimately linked to its material properties, which ultimately determines the potential applications of it.

The development of methods for the polymerization of alkene monomers are mainly focused on achieving fine control over macromolecular architectures, especially chain composition, molecular weight, and stereochemistry, already in the polymerization process; this allows for the synthesis of "high performance polyolefins", with virtually new properties or unusual combinations of them; in fact, since the discoveries of Ziegler and Natta [2,3], considerable efforts have been reported concerning the control of comonomer incorporation as well as dramatic improvements in activity.

One of the most powerful tool capable of providing high control over polymer architecture is living polymerization [4] catalyzed by transition metal complexes. Basically, a living system retains its ability to propagate the polymer chain and grow to a desired molar mass while its degree of termination or chain transfer is negligible.

This method allows both precise molecular weight control as well as the synthesis of a wide range of polymer architectures that were inaccessible just a decade ago. Moreover, these living polymers have the potential to be excellent compatibilizers, modifiers, additives, and elastomers.

While extraordinary advances in living/controlled polymerization have been made for anionic, cationic, and radical processes, there is a lack of living olefin polymerization systems. Indeed, olefin polymerization catalysts have always been inferior to their other chain-growth counterparts in this respect. The principal reason is that olefin polymerization catalysts always undergo irreversible chain transfer to metal alkyls and β-elimination reactions (Scheme 1.1). A significant number of advances have been made in the last decade and nowadays systems are available that have acceptable rates of propagation without appreciable chain transfer or termination.

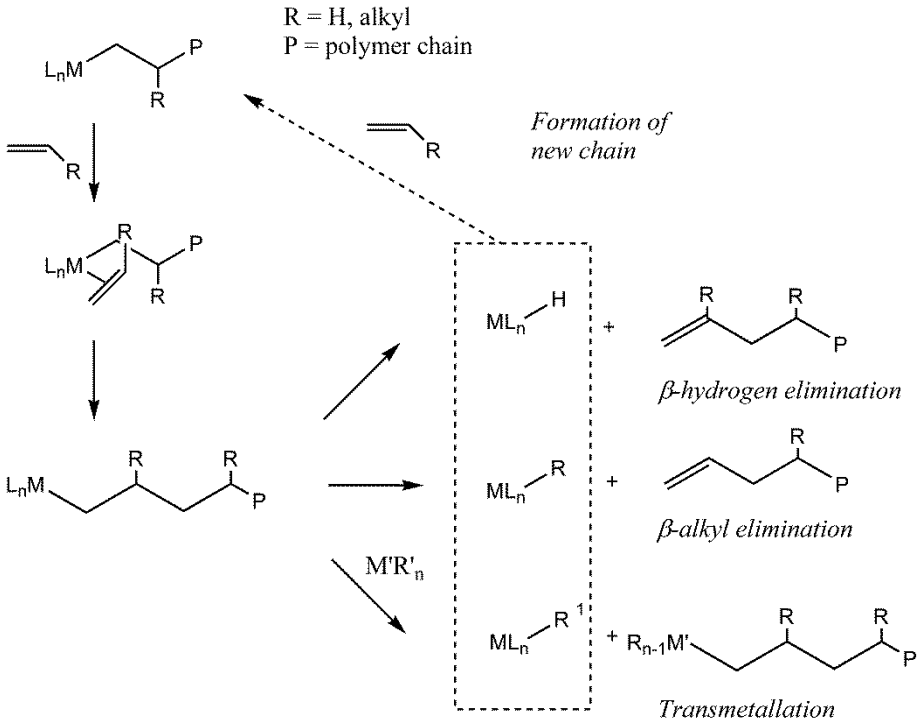


**Scheme 1.1.** *Propagation and chain transfer mechanisms in Ziegler-Natta olefin polymerization.*

## 1.2 Living polymerization: general considerations

Living olefin polymerization is one of the most useful tools for providing access to precisely controlled polymers such as monodisperse polymers, terminally functionalized

polymers, and block copolymers. These polymers are expected to display unique material properties that have not been achieved by conventional polymers.

There are seven generally accepted criteria for a living polymerization [5]:

1. polymerization proceeds to complete monomer conversion, and chain growth continues upon further monomer addition;
2. number average molecular weight ($M_n$) of the polymer increases linearly as a function of conversion;
3. the number of active centers remains constant for the duration of the polymerization;
4. molecular weight can be precisely controlled through stoichiometry;
5. polymers display narrow molecular weight distributions, quantitatively described by the ratio of the average molecular weight ($M_n/M_w \sim 1$);
6. block copolymers can be prepared by sequential monomer addition;
7. end functionalized polymers can be synthesized.

Common features of alkene polymerization catalyst systems are chain transfer and elimination reactions that terminate the growth of a polymer chain and result in the initiation of a new polymer chain by the catalyst. In metallocene catalyst, for example, consecutive alkene insertion into the metal carbon bond connecting the catalyst and the polymer chain proceeds until β-hydrogen elimination and/or transfer to the aluminum center. In contrast to late transition metal complexes, catalysts based on early transition metals are less prone to β-hydride eliminations, and so they can be more suitable to give living systems.

Several strategies have been devised to decrease the rate of chain termination relative to that of propagation such that catalytic systems can be living. For example, it is possible to simply lower the polymerization temperature to achieve at least a controlled behavior. Since β-hydrogen elimination process is unimolecular while propagation can be bimolecular, a lowering in temperature can more adversely affects elimination process.

## 1.3 Living propylene polymerization

### 1.3.1 Vanadium acetylacetonoate catalysts

In 1960s, Natta [6] discovered first that vanadium tetrachloride with $Et_2AlCl$ in the presence of propylene gave syndio-enriched polypropylene (Figure 1.1), at -78 °C.

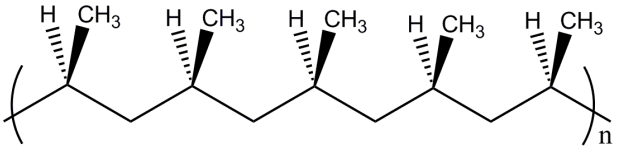


isotactic polypropylene

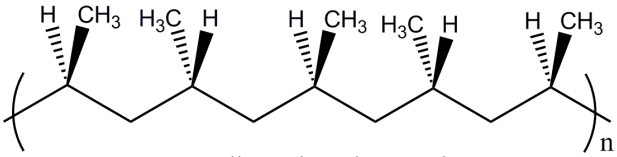


syndiotactic polypropylene

**Figure 1.1.** *Isotactic and syndiotactic polypropylene.*

After him, Doi's pioneering work [7] reported of $[V(acac)_3]/Et_2AlCl$ as a living catalyst for syndio-enriched PP ([*r*] = 0.81), at -65 °C. The resultant polymers exhibited narrow molecular weight distributions (PDI ~ 1.07-1.18) with a linear increase in $M_n$ with time even after 15 hours, giving polymers with $M_n$ of about 100.000 g/mol. However, slightly above -65 °C, the living behavior was diminished as evidenced by an increase in molecular weight distribution (at -48 °C, $M_w/M_n$ = 1.37-1.45). The activity and productivity was very low, and only 4% of the catalyst was active. Doi proved that the living behavior was also influenced by the alkyl aluminum co-catalyst identity: the more electron deficient $EtAlCl_2$ for example gave much broader molecular weight distribution, around 2.

### 1.3.2 Metallocene-based catalysts

Since the discovery of their catalytic activity, Group 4 metallocene complexes have found extensive use as olefin polymerization catalysts.

However, due to their high propensity towards eliminations via chain-transfer, there have been few examples of living olefin polymerization using them.

It has been demonstrated that at low reaction temperatures chain termination via β-H transfer can be suppressed and chain transfer to alkyl aluminum species can be avoided by

employing well-defined boron-based activators; some of the metallocene-based catalysts which promote living polypropylene polymerization are given in Figure 1.2.

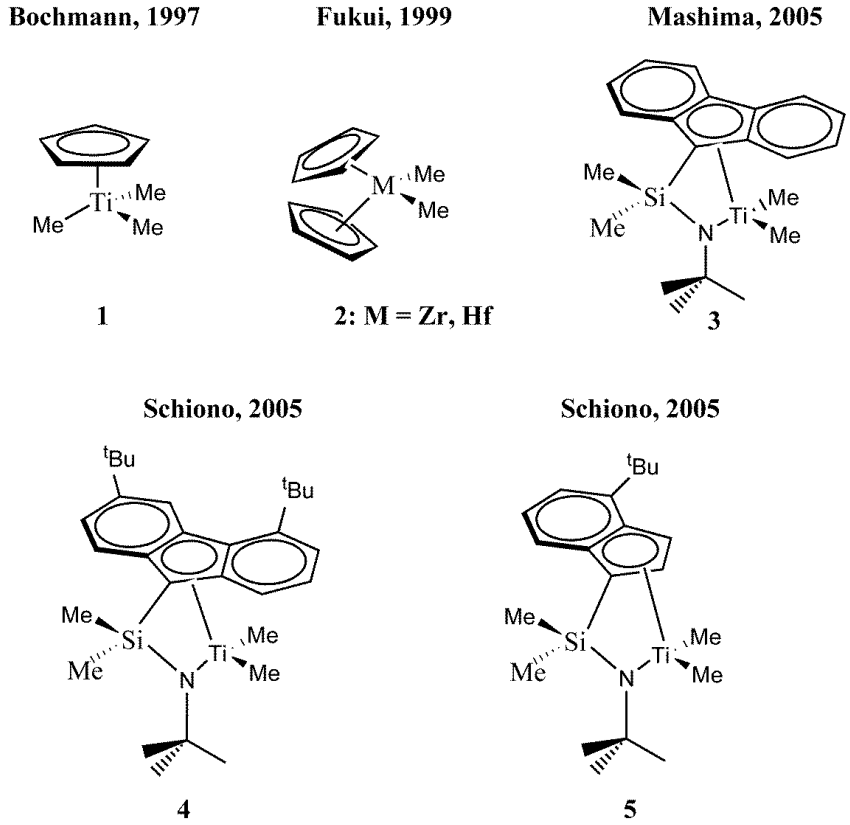


**Figure 1.2.** *Metallocene catalysts promoting living polypropylene polymerization.*

Bochmann [8] reported that complex **1**, upon activation with $B(C_6F_5)_3$ produced atactic high molecular weight PP with elastomeric properties, always with a linear increase in molecular weight with time. ($M_w$ = 1.103.000 g/mol and $M_w/M_n$ = 1.4 at -20 °C in toluene). From GPC analysis, it was estimated that 48 % of the polymer was composed of PP with narrow molecular weight distribution ($M_w/M_n$ = 1.10). Living PP polymerization has also been exhibited by bis-Cp type Group IV metallocenes at low temperatures. Fukui [9] reported that complex $[Cp_2ZrMe_2]$ (**2**) activated with $B(C_6F_5)_3$ in the presence of Al(*n*Oct)$_3$ as a scavenger, produces PP with $M_w/M_n < 1.15$, at -78 °C ($M_n$ = 9.400-27.300 g/mol). While at -50 °C, the molecular weight distribution broadens ($M_w/M_n$ = 1.55), the hafnium analogue produces PP with $M_w/M_n \sim$ 1.05-1.08 and $M_n$ = 6000-34.300 g/mol). In similar conditions, the titanium complex **3**, bearing monocyclopentadienyl-amido ligand, produces low molecular weight syndio-enriched PP ([*rr*] 0.49; $M_n$ = 9.800-19.900 g/mol with $M_w/M_n$ of 1.15-1.17) [10].

In an effort to find a system capable of forming highly syndiotactic PP in a living fashion, Shiono screened half-metallocene complexes bearing fluorenyl-based ligands [11]. Complex **4**, when activated with *d*-MAO at 0 °C, produces highly syndio-PP ([*rr*]~0.93) and PDI was 1.45, while employing an indenyl-based ligand (**5**) affords quasi-living PP polymerization [12]. In summary, the living character of the metallocene-based catalysts is only retained at low temperature. Generally, the molecular weight is relatively low or broader molecular weight distributions are observed.

### 1.3.3 Bis(phenoxyimine)titanium catalysts

Recent advances in the rational design and synthesis of well-defined transition metal complex catalysts for olefin polymerization have resulted in the discovery and development of quite a few efficient and selective catalysts for the living polymerization of ethylene, propylene, 1-hexene, or other olefins.

Fujita and coworkers at Mitsui Chemicals in 1999 reported on a class of Group IV complexes (Figure 1.3) bearing chelating phenoxyimine ligands [13] for the controlled (co)polymerization of olefinic monomers (now known as FI catalysts); if activated with MAO, these complexes showed extremely high activity first for ethylene polymerization [14], including selective vinyl- and Al-terminated polyethylenes, well defined PEs, and then they were found capable of producing a wide variety of unique polymers, including, highly isotactic and syndiotactic polypropylenes (*i*PPs and *s*PPs), and regio- and stereoirregular high molecular weight poly(higher –olefin)s [15].

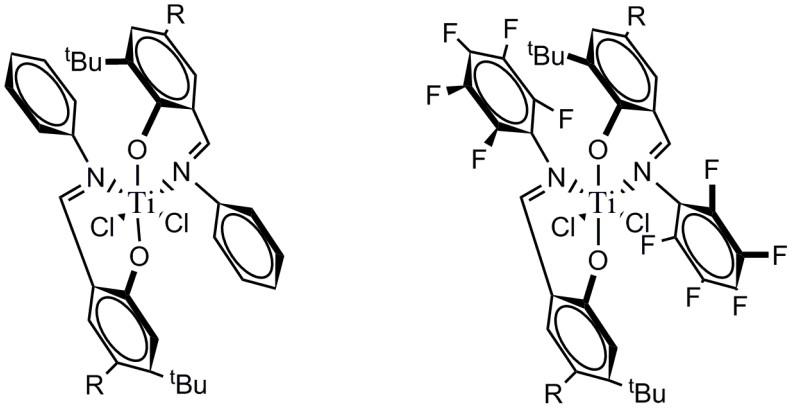


**6: R = H** **8: R = H**
**7: R = $^t$Bu** **9: R = $^t$Bu**

**Figure 1.3** *Early bis(phenoxyimine) titanium complexes.*

In contrast to the non-fluorinated analogue **7** [16], the incorporation of fluorinated N-aryl moieties into the bis(phenoxymine) ligand framework could provide catalyst precursors for syndiotactic and living PP [17]. The polymerization reaction with catalyst **8** gives low polydispersity ($M_w/M_n$ = 1.11) and a linear increase of $M_n$ with polypropylene yield, even if this trend deviates at higher molecular weights. The living behavior was further exemplified by the ability of making block copolymers. Worth noting, living behavior was still retained at 20 °C. Fujita [18] also reported that **9**/MAO gives also PP at room temperature, with $M_w/M_n$ = 1.07-1.14 and $M_n$ = 28500-108.000 g/mol. The complex activated with a supported cocatalyst has also been screened for propylene polymerization: **9**/$MgCl_2$/*i*-$BuAl(OR)_{3-n}$ gave polypropylene with narrow PDIs ($M_w/M_n$ = 1.09-1.17, $M_n$ = 53.000-132.000 g/mol) and a linear increase of with reaction time [19].

Recently, many new bis(phenoxymine)-based titanium complexes have been synthesized and screened; leading to new catalysts with variations on the N-aryl and phenoxide moieties (Figure 1.4).

Studies on the effect of the fluorination pattern of the N-aryl ring have been conducted [20] and it has been revealed that complexes bearing 2,4-di-tert-butyl phenoxyde moiety require at least one *ortho* fluorine on the N-aryl ring to exhibit living PP polymerization behavior.

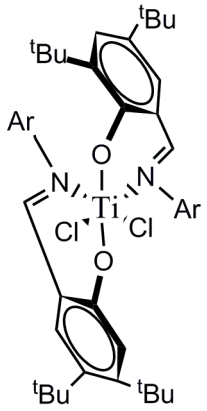


**10: Ar = 2-$FC_6H_4$**
**11: Ar = 2,6-$F_2C_6H_3$**
**12: Ar = 2,4,6-$F_3C_6H_2$**
**13: Ar = 2,3,5,6-$F_4C_6H$**
**14: Ar = 2,3,5,6-$F_4$-4-$CF_3C_6$**

**Figure 1.4.** *Bis(phenoxyimine) titanium complexes with varying N-aryl fluorine substitution patterns.*

The PP produced by **12**/MAO is highly tactic ([*rrrr*] 0.95), while **11**/MAO produces a polymer that is less stereoregular ([*rrrr*] 0.83). Notably, tacticity drops off significantly upon moving to the monofluorinated complex **10** which affords polypropylene with [*rrrr*] 0.52. It was reported that **14**/MAO was 1.5 times more active

than **8**/MAO for PP polymerization and still able to provide highly syndiotactic polymer with narrow molecular weight distribution [21].

One recent variation [20] to the bis(phenoxyimine) complexes involves the coordination of two different phenoxyimine ligands to one titanium center, as reported in Figure 1.5. Using pooled combinatorial approach, several heteroligated complexes bearing both a "living" and "non-living" ligand were synthesized and screened for propylene polymerization.

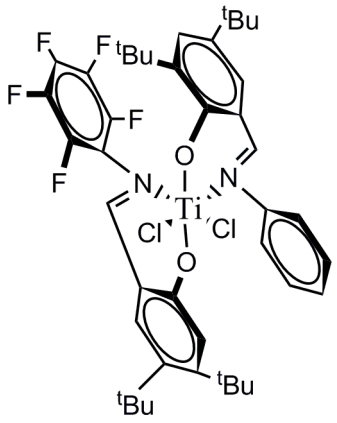


**15**

**Figure 1.5.** *Heteroligated bis(phenoxyimine) titanium complex.*

The molecular weight distribution of the resulting polymers formed from mixed catalysts fell between those of the corresponding homoligated catalysts, the activity was significantly higher in some cases. For example, PP produced with **7**/MAO exhibithed broad PDI ($M_w/M_n$ = 1.41) and a turnover frequency of 42 $h^{-1}$ while **8**/MAO showed narrow PDI ($M_w/M_n$ = 1.06) and a turnover frequency of 221 $h^{-1}$. However, the heteroligated catalyst **15**/MAO (Figure 1.3) produced PP with $M_n$ = 70.170 g/mol, $M_w/M_n$ = 1.16 and exhibited a turnover frequency of 760 $h^{-1}$, giving syndiotactic PP.

### 1.3.4 Bis(phenoxyketimine)titanium catalysts

Bis(phenoxyimine) titanium complexes produce *s*PP through a chain-end control mechanism despite the fact that the catalyst precursors are $C_2$-symmetric in the solid state and in solution. The reason for this phenomenon stems from a proposed ligand isomerization event that provides enantiomeric coordination sites. It has been proposed that placing a substituent at the imine carbon of the phenoxyimine ligand could prevent this isomerization and lead to the formation of *i*PP [22].

Ketimine complexes were therefore synthesized (Figure 1.6) and while they were shown to polymerize ethylene in a living fashion upon activation, they proved to be sparingly active for propylene polymerization [23]. It was reasoned that the reduction of the size of the *ortho* substituents of the phenoxyde moiety could provide a sterically less encumbered active site potentially enabling higher activities for propylene polymerization.

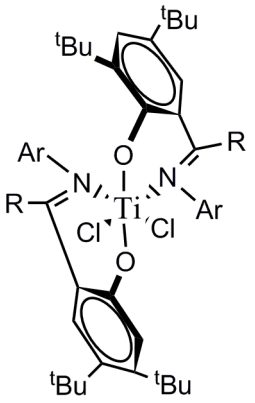


**16: R = Me**
**17: R = Et**
**18: R = Ph**

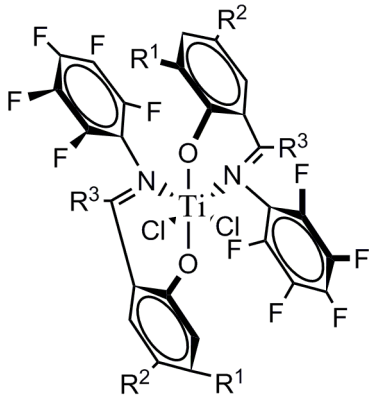


| | $R^1$ | $R^2$ | $R^3$ |
|---|---|---|---|
| **19** | $^i$Pr | $^i$Pr | Ar |
| **20** | Et | Me | Ar |
| **21** | Me | Me | Ar |
| **22** | H | Me | Ar |
| **23** | Me | Me | H |

**Figure 1.6.** *Bis(phenoxyketimine) titanium complexes.*

Complex **19-23** were screened for propylene polymerization. Upon activation with MAO at 0 °C, each of them produced PP with narrow PDI ($M_w/M_n$ = 1.12-1.17, $M_n$ = 2.700-35.400 g/mol) and **21**/MAO was capable to exhibit a linear increase in PP molecular weight as a function of yield [22].

## 1.4 Living ethylene polymerization

The range of different polymer architectures derived from the simple ethylene is really intriguing. The properties of PEs vary greatly depending on the polymer microstructure from high density to low density, branched materials. The most early transition metal olefin polymerization catalysts furnish linear PE, while late transition catalysts typically give rise to branched structures [24].

### 1.4.1 Non-group 4 metal polymerization catalysts

Apart from the Group 4 metal complexes, examples with group 3, group 5 and late transition metals have been reported as regards living ethylene polymerization.

#### 1.4.1.1 Group 3 metal polymerization catalysts

The potential of f-block metal complexes to serve as living olefin polymerization catalysts was demonstrated by Marks in 1985 [25].

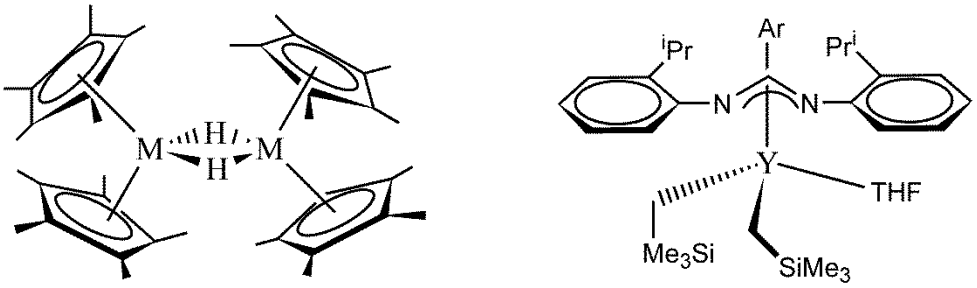


**24: M = La**
**25: M = Nd**
**26: M = Lu**

**27**

**Figure 1.7.** *Lanthanide and group 3 metal catalysts for living olefin polymerization.*

Dimeric bis(Cp*) hydride complexes of lanthanum, neodymium, and lutetium (**24-26**, Figure 1.7) were shown to polymerize ethylene with extremely high activities (up to 3040 g PE/mmol$^{-1}$ min$^{-1}$ atm$^{-1}$). The PEs exhibited high molecular weights ($M_n$ = 96.000-648.000 g/mol) with $M_w/M_n$ = 1.37-4.46. Further evidence in support of the living nature of ethylene polymerization includes the observations that catalytic activity is maintained at room temperature for up to 2 weeks, $M_n$ increases with increasing reaction time, and the number of polymer chains per metal center is consistently less than one which argues against chain-transfer followed by reinitiation.

Hessen [26] and coworkers reported on the synthesis and ethylene polymerization activity of dialkyl(benzamidinate)yttrium complexes which displayed some characteristics of living behavior. When treated with [$PhNMe_2H$][$B_8C_6F_5)_4$], complex **27** catalyzed the formation of PE. The final polymer possessed narrow molecular weight distribution ($M_w/M_n$ = 1.1-1.2) and high molecular weights ($M_w$ = 430.000-1.269.000 g/mol). Moreover, it was shown that about 1.1 polymer chains per metal center were produced and

this number was constant over the course of 30 minutes. Taken together, these observations suggest that **27** is living for ethylene polymerization.

### 1.4.1.2 Group 5 metal polymerization catalysts (V, Nb; Ta)

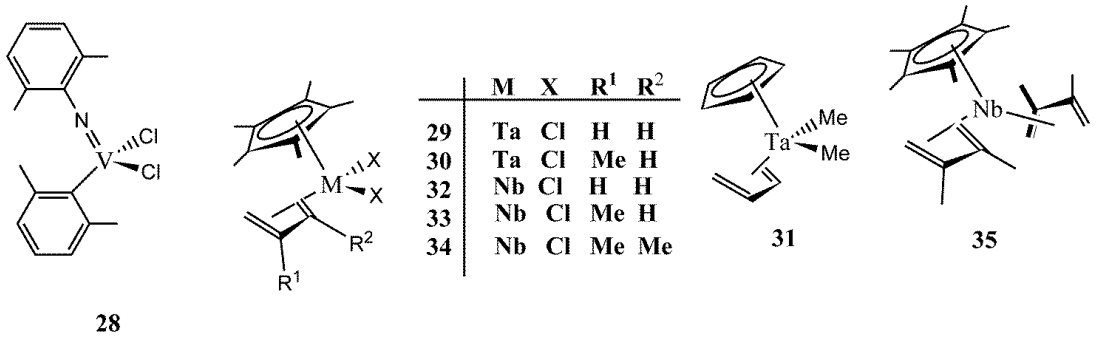


| | M | X | $R^1$ | $R^2$ |
|---|---|---|---|---|
| 29 | Ta | Cl | H | H |
| 30 | Ta | Cl | Me | H |
| 32 | Nb | Cl | H | H |
| 33 | Nb | Cl | Me | H |
| 34 | Nb | Cl | Me | Me |

**28** **31** **35**

**Figure 1.8.** *Niobium and tantalum complexes for living ethylene polymerization.*

Nomura and coworkers [27] reported that arylimido(aryloxo)vanadium dichloride complexes activated with $Et_2AlCl$ exhibited characteristics of living ethylene polymerization (Figure 1.8). In particular, **28**/$Et_2AlCl$ furnished PE with narrow molecular weight distribution ($M_w/M_n$ =1.42) and high molecular weight ($M_n$ = 2.570.000 g/mol) at 0 °C.

Examples of living ethylene polymerization by Group 5 metal complexes are not limited to those based on vanadium. In fact, in 1993, Nakamura [28] reported on the synthesis and ethylene polymerization behavior of cyclopentadienyl($\eta^4$-diene)tantalum complexes. Upon activation with MAO at temperatures of 20 °C or below, compounds **29-31** gave PEs with narrow molecular weight distributions ($M_w/M_n$ =1.4) with $M_n$ = 8.600-42.900 g/mol. Later [29], the analogous niobium complexes 32-35 were shown to behave in the same way up to 20 °C.

### 1.4.1.3 Group 5 metal polymerization catalysts (V, Nb; Ta)

Theopold and coworkers [30] investigated ethylene polymerization catalyzed by chromium complexes bearing 2,4-pentane-N,N'-bis(aryl)ketiminato ($(Ar)_2$nacnac) ligands as a potential model for ethylene polymerization by heterogeneous Philips catalysts. When exposed to ethylene at room temperature, complex **36** (Figure 1.9) formed polymer with $M_n$ = 10.000-110.000 g/mol and narrow molecular weight distributions ($M_w/M_n$ =1.17-1.4).

These results represented the first report of living ethylene polymerization with a chromium-based catalysts.

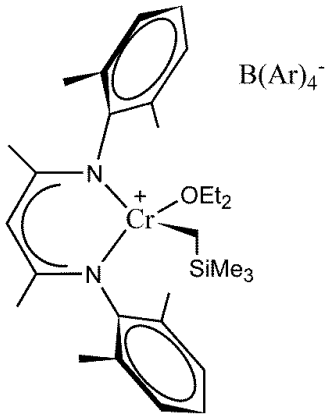


**36**

**Figure 1.9.** *β-diiminate chromium complex for living ethylene polymerization.*

### 1.4.1.4 Late transition metal polymerization catalysts

Brookhart and coworkers have used various Cp* cobalt complexes for the synthesis of end-functionalized PEs [31]. Reaction of **37-41** with 1 atm of ethylene in chlorobenzene for 3 h led to the formation of low molecular weight, aryl-substituted PEs with quite narrow molecular weight distributions ($M_n$ up to 21 200 g/mol, $M_w/M_n$ = 1.11-1.16).

Significant advances both in terms of increasing molecular weights and decreasing polydispersities of PE were achieved with palladium catalysts **42-43** (Figure 1.10) [32]. At 5 °C, highly branched (100 branches/1000 carbons), amorphous PEs with very narrow molecular weight distributions ($M_w/M_n$ = 1.1) were produced. Molecular weight distributions broadened somewhat at 27 °C for long reaction times. Pd diimine catalysts were further extended to generate both mono- and di-end functionalized, monodisperse, highly branched polyethylenes [33].

Use of ester-functionalized catalyst **42** allowed for preparation of branched polyethylenes with a methyl ester end group at the beginning of the chain. Further, a telechelic polymer could be produced by addition of alkyl acrylates before the silane quench. Acrylates undergo one insertion into the growing chain, forming stable chelates, but do not insert further, allowing for clean end-functionalization without block formation. With this method it was possible to generate polymers with two distinct ester end groups.

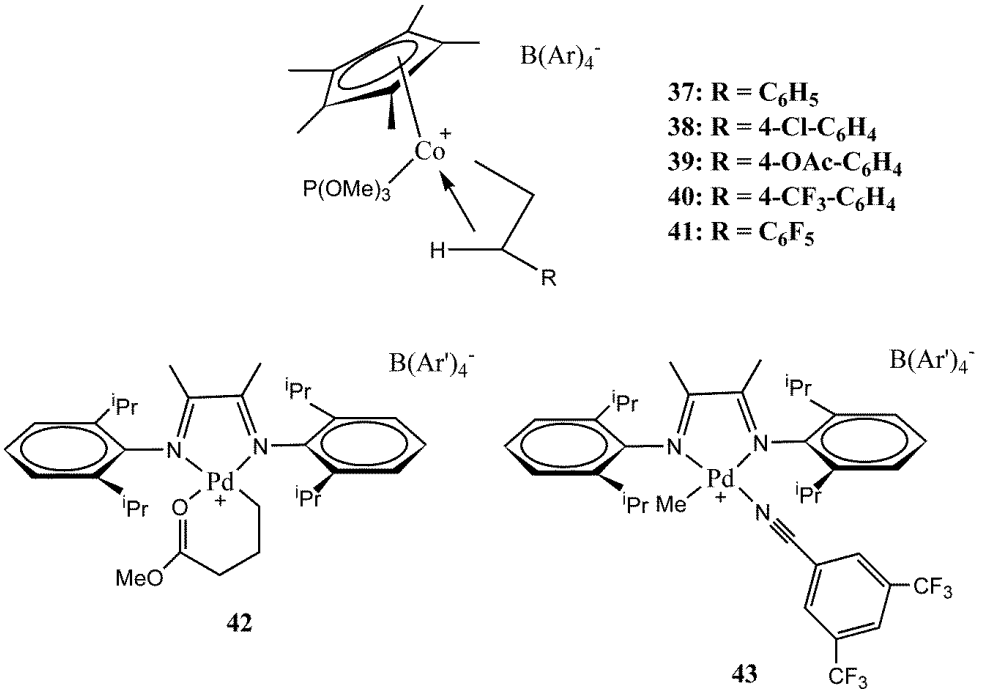


**Figure 1.10.** *Late transition metal catalysts for living ethylene polymerization.*

Guan and co-workers [34] have extended the study of hindered diimine catalysts with cyclophane complex **44** (Figure 1.11). When activated with MMAO, it is highly active for production of branched PEs (66–97 branches/1000 carbons) with relatively narrow polydispersities ($M_w/M_n$ as low as 1.23 at 50 °C). Most significantly, these catalysts exhibit impressive thermal stability, with good activities even up to 90 °C. However, the polydispersities increase, and the activities decrease somewhat at higher temperatures.

In order to circumvent the above-mentioned instability of conventional Ni α-diimine catalysts, Brookhart and co-workers [35] have investigated a series of anilinotropone-based nickel catalysts **45-47**. With activation by $Ni(COD)_2$, high activities and long lifetimes were observed, particularly in the aryl-substituted cases, **46-47** (Figure 1.11). The $M_n$ was shown to increase in nearly linear fashion with time, suggesting minimal chain transfer. PDIs were relatively narrow (as low as 1.2 at room temperature), but increased at higher temperatures and with longer reaction times.

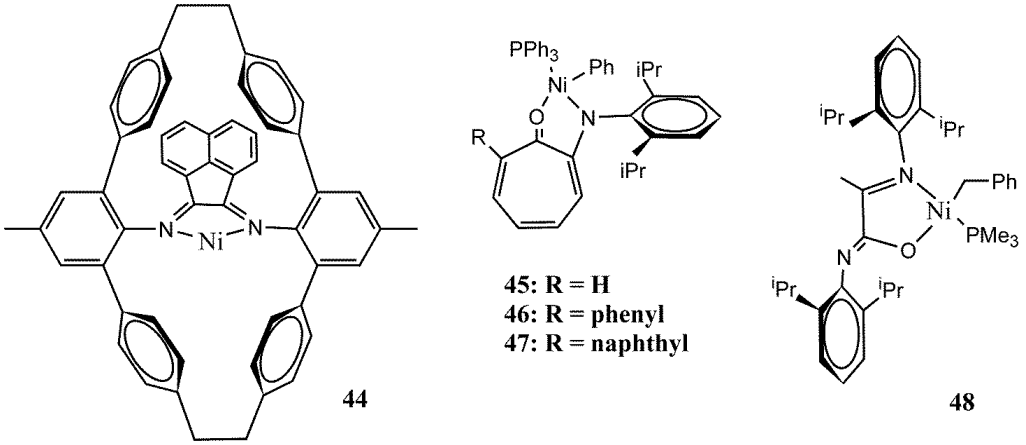


**Figure 1.11.** *Ni complexes for living polymerization.*

Bazan and co-workers have observed quasi-living ethylene polymerization behavior with nickel diimine variant **48** (Figure 1.11) [36]. With $Ni(COD)_2$ as activator, $M_n$ increased linearly with time up to 30 min at 20 °C, producing a PE with low branching (12-19 methyl branches/1000 carbons). Molecular weight distributions were as low as 1.3, somewhat larger than expected for a truly living system, which the authors attribute to a slow initiation, or to precipitation of the product.

### 1.4.2 Bis(phenoxyimine)titanium catalysts

It has been shown that incorporation of *ortho*-fluorinated N-aryl moieties into the bis(phenoxyimine) framework is typically required to obtain catalysts that are living for propylene polymerization. The living polymerization of ethylene has been reported with many of the same catalysts. For example, two of the earliest bis(phenoxyimine) titanium complexes reported for living syndiospecific propylene polymerization, **8** and **9** (Figure 1.3), have also been shown to polymerize ethylene in a living fashion. In 2001, Fujita [37] and co-workers reported that at 25 °C, **9**/MAO polymerized ethylene to produce linear PE with a high molecular weight and narrow molecular weight distribution ($M_n$ = 412.000 g/mol, $M_w/M_n$ = 1.13). Furthermore, polymerizations at 25, 50 and 75 °C exhibited a linear increase in $M_n$ with reaction time although, at 75 °C, molecular weight distributions broadened with longer reaction times ($M_w/M_n$ = 2.05 at 15 min). As previously discussed, some of the earliest group IV bis(phenoxyimine) complexes, including **6** (Figure 1.3 and its zirconium analogue) have been shown to be precursors for highly active ethylene polymerization catalysts **14**. In 2003, Coates and co-workers reported that **7**/MAO polymerized ethylene at 50 °C to produce polyethylene with $M_n$ = 44.500 g/mol and $M_w/M_n$

= 1.10; the measured molecular weight of the polymer matched well with the theoretical value [23]. The ability of **6** to polymerize ethylene in a living fashion was reported later. Fujita and co-workers reported on ethylene polymerization behavior with the same system and found that while molecular weight distributions were low at a reaction time of 1 min ($M_w/M_n$ = 1.12, $M_n$ = 52.000 g/mol), the molecular weight distribution broadened significantly at reaction times of just 5 min ($M_w/M_n$ = 1.61, $M_n$ = 170.000 g/mol) [38].

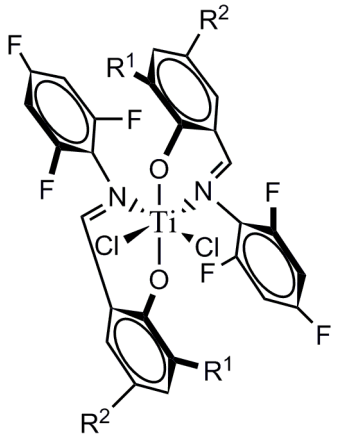


**49: $R^1$ = $CMe_2Ph$; $R^2$ = Me**
**50: $R^1$ = $^tBu$; $R^2$ = H**

**Figure 1.12.** *Bis(phenoxyimine) titanium catalyst precursors for living ethylene polymerization.*

While **49**-**50**/MAO (Figure 1.12) produced amorphous polypropylene with bimodal GPC traces, each of these catalysts has been shown to be well-behaved for ethylene polymerization at 50 °C and **49**/MAO and **50**/MAO produced polymers with narrow molecular weight distributions at reaction times between 1 and 5 min ($M_w/M_n$ = 1.05, $M_n$ = 13.000-64.000 g/mol) [39]. Lastly, Fujita and co-workers reported that $ZnEt_2$ could be used as a chain-transfer agent in the living ethylene polymerization employing **49**/MAO [40]. In this system, a living PE chain-end reacts with $ZnEt_2$ only after all ethylene has been consumed. This leads to a zinc end-functionalized polymer chain and a titanium species that is able to grow another living chain upon addition of monomer.

When **49** is employed, residual $ZnEt_2$ does not appear to interfere with the second stage of the polymerization as PDI values for the final polymer are low. However, the authors found that when **50** is used in this system, the second stage of the polymerization was no longer living as the $ZnEt_2$ appeared to react with the living chain-end despite the presence

of monomer. It was concluded that the nature of the *ortho*-phenoxide substituent was crucial in dictating reactivity between the polymer chain-end and $ZnEt_2$.

### 1.4.3 Bis(phenoxyketimine)titanium catalysts

While bis(phenoxyketimine) titanium complexes that have a bulky substituent *ortho* to the phenoxide-bearing carbon show very low activity for propylene polymerization, such complexes, upon activation, can polymerize ethylene in a living fashion. For example, Coates and co-workers reported that at 0 and 20 °C, **16-18**/MAO (Figure 1.6) all produced PE that exhibited a narrow molecular weight distribution ($M_w/M_n$ = 1.08) and had number average molecular weights ($M_n$ = 15.000–47.000 g/mol) that coincided with theoretical values [23].

Furthermore, additional experiments demonstrated a linear increase in $M_n$ with polymer yield for the polymerization catalyzed by **18**/MAO at 0 °C and for **17**/MAO at 50 °C.[23] It was also shown that a related complex (**51**, Figure 1.13), when activated with MAO at 50 °C, produced PE with $M_w/M_n$ = 1.08 ($M_n$ = 9.000 g/mol) [41].

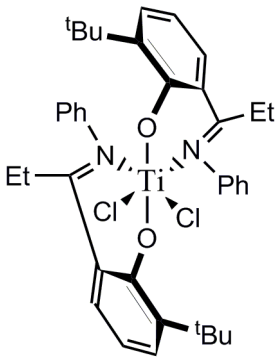


**51**

**Figure 1.13.** *Bis(phenoxyketimine) titanium catalyst precursor for living ethylene polymerization.*

### 1.4.4 Titanium indolide-imine catalysts

As the bis(phenoxyimine)titanium complexes exhibited good living propylene and ethylene polymerization properties, Fujita and co-workers synthesized structurally similar bis(indolide-imine)- titanium complexes and evaluated their potential as ethylene polymerization catalysts [42]. When activated with MAO in the presence of ethylene at room temperature, compounds **52-54** (Figure 1.14) furnished PE with narrow molecular

weight distributions ($M_w/M_n$ = 1.11-1.23) with $M_n$ = 11.000-90.000 g/mol. Ethylene polymerization by **54**/MAO exhibited a linear increase of $M_n$ with increasing polymer yields. The catalyst system comprised of **54**/MAO also showed impressive thermal stability in that the PE obtained at 50 °C retained a narrow PDI value of 1.24. In a subsequent report, it was shown that exhaustive fluorination of the N-aryl moiety (**55**) had deleterious effects on the living character of ethylene polymerization [42]. The PE produced by **55**/MAO at 25 °C possessed a broadened molecular weight distribution relative to the polymers produced by **52-54**/MAO under identical conditions (**55**: $M_w/M_n$ = 1.93). The polymerization activity of **55**/MAO was much higher than those for **52-54**/MAO. Upon lowering the temperature to 10 °C, ‘‘quasi-living behavior’’ was observed; the $M_n$ was shown to increase linearly with time over the course of 6 min, and the molecular weight distribution decreased to give $M_w/M_n$ = 1.12-1.15. No evidence for chain transfer to aluminum or β−H transfer was observed.

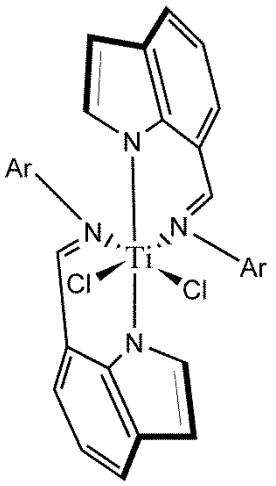


**52: Ar = Ph**
**53: Ar = 2-6-$F_2$-$C_6H_3$**
**54: Ar = 2,4,6-$F_3$-$C_6H_2$**
**55: Ar = $C_6F_5$**

**Figure 1.14.** *Bis(indolide-imine) titanium catalysts.*

### 1.4.5 Bis(enaminoketonato)titanium catalysts

There are a myriad of examples of homogeneous olefin polymerization catalysts based on titanium, and a significant portion of these exhibits living behavior. The most prolific classes of living, titanium-based olefin polymerization catalysts bear ligands containing nitrogen and oxygen donors. In line with this observation, Li and co-workers [43] reported on the synthesis and ethylene polymerization activity of bis(enaminoketonato)titanium complexes. Upon activation with MAO in the presence of ethylene at 25 °C, **56-57** (Figure 1.15) furnish linear PEs with narrow molecular weight

distributions ($M_w/M_n$ 1.25-1.45) and $M_n$ = 51.000-129.000 g/mol. A linear increase in $M_n$ with reaction time is observed for the polymerization catalyzed by **56**/MMAO at 25 °C. The ethylene polymerization activity is greatly affected by the substitution pattern of the ligand backbone with higher activities being obtained in the cases where the electron-withdrawing $CF_3$ moiety is incorporated (**56**: 1.32 kg/mmol[Ti] h, **60**: 0.12 kg/mmol[Ti] h).

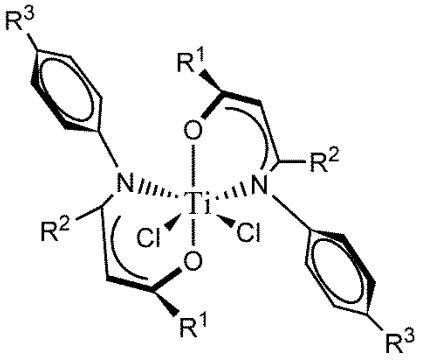


| | $R^1$ | $R^2$ | $R^3$ |
|---|---|---|---|
| **56** | **Ph** | **$CF_3$** | **H** |
| **57** | **2-thiophenyl** | **$CF_3$** | **H** |
| **58** | **2-furanyl** | **$CF_3$** | **H** |
| **59** | **$CF_3$** | **$CH_3$** | **H** |
| **60** | **Ph** | **$CH_3$** | **H** |

**Figure 1.15.** *Bis(enaminoketonato) titanium complexes for living olefin polymerization.*

### 1.4.6 Bis(enolatoimino)titanium catalysts

A new type [44] of Ti complexes with imineenolato ligands for living ethylene polymerization was introduced by Mecking (**64**) and it is reported in Figure 1.16:

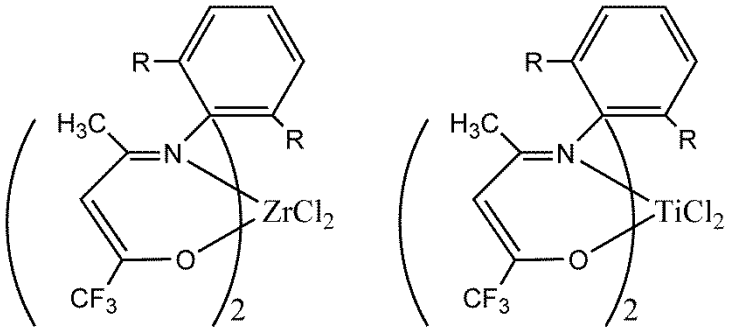


**63a: R = H** **64a: R = H**
**63b: R = F** **64b: R = F**

**Figure 1.16.** *Enolatoimino zirconium and titanium complexes.*

The catalyst system **64b** displayed high activities and produces high molecular weight polyethylenes with MAO as a cocatalyst at room temperature under atmospheric pressure. With a new *ortho*-fluorinated titanium imineenolato complex (**63a**), ethylene is

polymerized in an unprecedented living fashion affording polymer with a high molecular weight ($M_n > 10^5$ g mol$^{-1}$) and an extremely narrow distribution ($M_w/M_n = 1.01$) at the same time; the living character is also retained even at an elevated temperature of 75°C ($M_w/M_n$ = 1.15 after 15 min) and even after 1h of polymerization time ($M_n$ = 9.9 x $10^5$ g mol$^{-1}$, $M_w/M_n$ = 1.17 at 25 ºC). The polymer molecular weight determined agrees within experimental error with the theoretical value calculated from the amount of polymer obtained and catalyst precursor employed. This shows that the catalyst precursor is rapidly converted to a single type of active species, chains are initiated simultaneously, and essentially no chain transfer or termination occurs. Ethylene/propylene block copolymers were also accessible.

In contrast, complexes **64a**, lacking fluorine atoms in the *ortho*-position, did not promote any living ethylene polymerization and a comparatively much broader polydispersity ($M_w/M_n$ = 1.45) is observed; the catalyst precursor is incompletely activated.

Mecking also synthesized the enolatoimino Zr complexes **63** [45]; even if activation with MAO gave linear polyethylene with high molecular weight, unlike the titanium analogue **64b**, the polymerization with **63b**/MAO did not occur in a living fashion.

## 1.5 Living homo- and copolymerization of cyclic olefins

### 1.5.1 Introduction

There is tremendous interest in cycloolefin homo- and co-polymers, because of easy availability of the monomers and interesting polymer properties. Homopolymers of cyclic olefins (e.g. polynorbornene, Figure 1.17) are characterized by extremely high melting points which are usually greater than their decomposition temperature, and by low solubility in most organic solvents. For these reasons, they are difficult to process and therefore commercially insignificant. However, upon incorporation into copolymers with α-olefins, it is possible to obtain materials with desirable properties. In fact, the presence of non-cyclic units introduces flexibility in the polymer chain. Thus, the copolymers are processable, and soluble in most organic solvents.

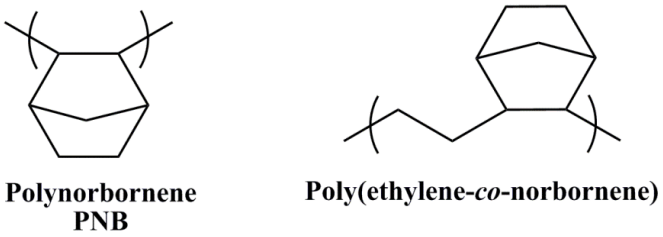


**Figure 1.17.** *Homopolymers and copolymers of norbornene.*

In addition to high glass temperature of the rigid polycyclic backbone, norbornene offers other very attractive properties such as low moisture uptake, low dielectric constant, low dielectric loss, high breakdown voltage, chemical resistance, and a wide spectral window.

In the early 1960s, cycloolefins such as norbornene could be polymerized by heterogeneous systems based on titanium, tungsten, or molybdenum halides with strong Lewis acidic cocatalysts; the polymerization occurred via ring opening [45]. After that, the discovery [47] of single site catalysts has revolutionized norbornene homo- and co-polymerization, leading to novel cycloolefin polymers for applications as engineering resins, medical packaging and also new functional applications as waveguides, adhesives, photoresists and encapsulants for various electronic applications.

### 1.5.2 Mechanisms of cycloolefin homopolymerization

Cycloolefins give two different kind of coordination polymerization with metal catalysts, the Ring Opening Metathesis Polymerization (ROMP) and the addition polymerization, which are reported in Scheme 1.2.

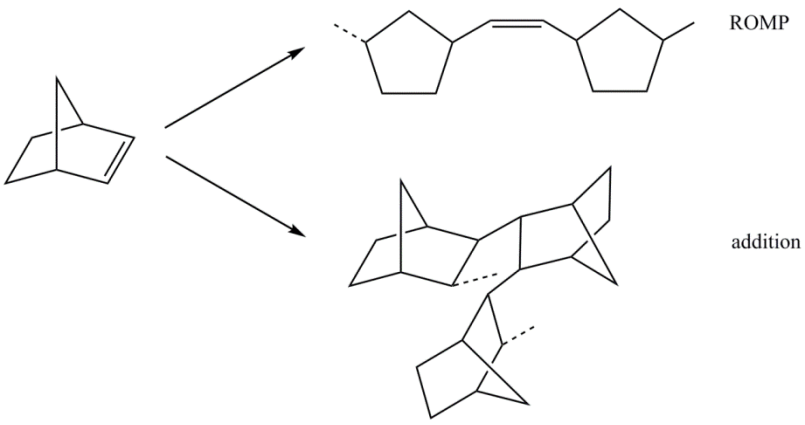


**Scheme 1.2.** *Schematic representation of norbornene coordination polymerization.*

### 1.5.2.1. ROMP Polymerization

The ROMP of cyclic olefins (e. g. norbornene) was described first in 1960 by DuPont [48]: toluene soluble polymers with olefinic insaturations were synthesized using $TiCl_4/LiAl(C_7H_{13})_4$ with Ti/Al = 0.5, while toluene insoluble saturated polymers were produced with Ti/Al = 2. After that, in 1970 Chauvin [49] recognized the role of metal carbene complexes and metallacyclobutane. Moreover, Höcker [50] and Thorn-Csànyi [51] investigated the complex equilibria involving cycloolefin monomers, macrocyclic ROMP oligomers, and linear polymers.

The better comprehension of ROMP process gave rise to novel single-site catalytic systems, especially the ones developed by Schrock [51] and Grubbs [52].

The ROMP reaction involves breaking and reforming olefin double bonds with the simultaneous opening of the unsaturated cycles of the monomers [53]. The reactivity of this cyclic olefin mainly depends upon the release of the strain energies[54] of the cyclic structure, the steric hindrance and the possibility of giving β-H elimination.

### 1.5.2.2. Addition polymerization

With addition polymerization, the bicyclic unit of the monomer remains the same and only the double bond is opened. The reaction is influenced by the ring strain of the cyclic olefin and by the non-planarity of the double bond: in fact, the out-of-plane double bond protons make the monomer insertion easier due to the lower barrier during the $sp^3$ hybridization.

Catalysts which give addition polymerization are early transition metals [55], zirconocenes in particular, palladium and nickel [56] and chromium and cobalt catalysts [57].

### 1.5.3 Living norbornene homopolymerization

Risse [59] has reported on the controlled norbornene polymerization with catalyst $[Pd(MeCN)][BF_4]_2$ obtaining saturated polymers; the reaction was not sensitive to added water, supporting an insertion mechanism rather than cationic propagation. Only for low conversion a renewed chain growth was observed with sequential monomer addition. At 0 °C, narrow molecular weight distributions were observed for short reaction times (t = 20 min; 54 % conversion; $M_n$ = 21.400 g/mol, $M_w/M_n$ = 1.07), but broadened as conversion increased ($M_w/M_n$ = 1.34 at 100 % conversion). Moreover, ester-functionalized norbornenes [60] were investigated: although the appended functionality was tolerated in

many cases, the reactivity was diminished. However, the relationship of molecular weight conversion percentage was linear and relatively narrow molecular weight distributions were obtained in many cases ($M_n$ as low as 1.15).

### 1.5.4 Living polymerization of ethylene and norbornene

#### 1.5.4.1 Introduction

E–N copolymers are usually amorphous and display a wide range of $T_g$, from room temperature to about 220 °C. They are characterized by high chemical resistance as well as good processability. They show excellent transparency and high refractive index, owing to their high carbon/hydrogen ratio, e.g., the refractive index is 1.53 for a 50:50 E–N copolymer. These properties make them suitable for optical applications such as coatings for high-capacity CDs and DVDs, for lenses, medical equipment, blisters, toner binder, and packaging. The industrially produced copolymers have norbornene contents between 30 and 60 mol % and $T_g$ values of 120-180 °C.

E–N copolymers have been developed to commercial products such as TOPAS from Ticona [61,62], while Mitsui produces APEL by using vanadium-based catalysts [27,63].

#### 1.5.4.2. E-N Copolymers Microstructure

The properties of E-N copolymers depend on comonomer composition, the distribution of monomers along the chain, and on the chain stereoregularity. which are determined by the structure of the catalyst precursor and their microstructure has only recently undergone a detailed investigation using $^{13}C$ NMR spectroscopy [64], that is the most powerful tool for polymer microstructural investigation. E-N copolymers' spectra are quite complex for the presence of two stereogenic carbons per norbornene unit; moreover, the chemical shifts do not follow additive rules, because of the bicyclic nature of the monomer units.

Norbornene showed to be enchained by *cis*-2,3-*exo* addition [47] and since one β-hydrogen is located on the *endo* side and *trans* to the Metal-C bond it does not undergo β-hydrogen elimination; in Figure 1.18 the sequence EENEE is reported, together with the carbon atoms numbering.

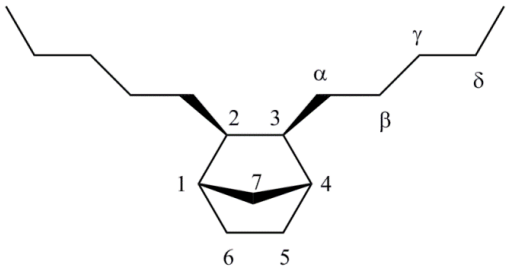


**Figure 1.18.** *E–N copolymer segment (EENEE) with an isolated norbornene unit.*

Moreover, in Figure 1.19 possible configurations of E-N sequences are reported: norbornene units can be alternated (ENENE), diads (ENNE) or triads (ENNNE).

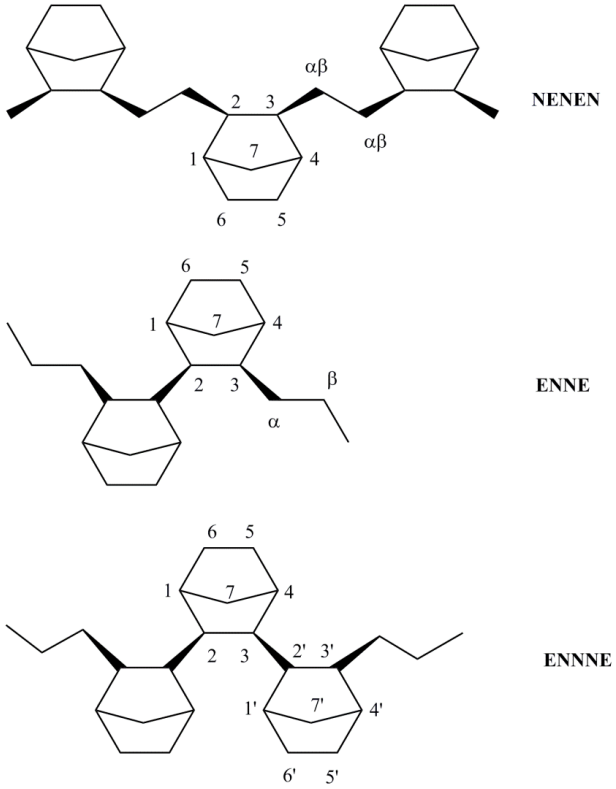


**Figure 1.19.** *Segments of E–N copolymer chain with norbornene in alternating (NENEN), diad (ENNE) and triad (ENNNE) sequences.*

The $C_2/C_3$ atoms configuration can be S/R or R/S, therefore the relationship between two subsequent norbornene units can be erythrodiisotactic (*meso*) or erythrodisyndiotactic (*racemic*); the possible stereochemical configurations are reported in Figure 1.20.

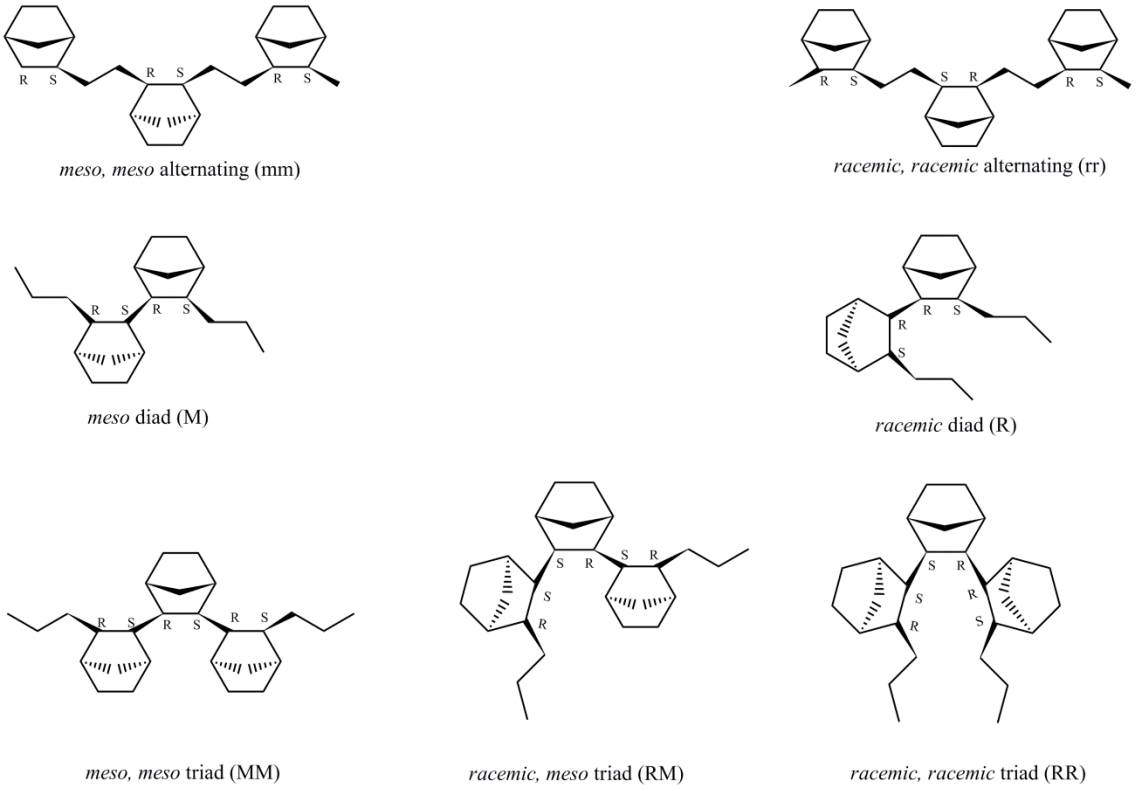


**Figure 1.20.** *Alternating (NENEN), diad (ENNE) and triad (ENNNE) sequences, showing the possible configurations.*

### 1.5.5 Catalysts for living ethylene-norbornene polymerization

Catalyst **3**/MAO (Figure 1.2), which has been shown to polymerize propylene in a living manner, can also be used for living copolymerization of ethylene with norbornene. At 0 °C, it can produce E-N random copolymer with $M_n$ = 78.000 and $M_w/M_n$ = 1.15 [65]. In addition, a linear increase in $M_n$ with time was observed. Microstructural analysis by $^{13}C$ NMR revealed that the copolymer contained 53 mol % of norbornene and from DSC a $T_g$ of 166 °C was measured. In a later report [66], samples with higher $T_g$ values were synthesized with **3**/MAO (up to 185 °C) at 40 °C, but molecular weight distributions were broader ($M_w/M_n$ ~ 1.3). Similar compounds (Figure 1.2), when activated with MAO, also provided ethylene-norbornene copolymers with fairy narrow PDIs ($M_w/M_n$ = 1.21-1.27), even if norbornene content and thus $T_g$ values were lower ($T_g$ < 114 °C).

Shiono also reported the copolymerization of propylene and norbornene with **3**/MAO [67] to produce copolymers with high $T_g$ and narrow molecular weight distributions (for example, at 20 °C, **3**/MAO gave $M_n$ = 156.000 g/mol and $M_w/M_n$ =1.16; $T_g$ = 249 °C).

Living ethylene homopolymerization by Group 4 metallocene catalysts were reported by Tritto [68,69] and coworkers, they have shown that *rac*-Et(Ind)$_2$ZrCl$_2$/MAO (**65**), 90% *r*/10% *m*-Et(4,7-Me$_2$Ind)$_2$ZrCl$_2$ (**66**), and *r*-H$_2$C(3-*t*BuInd)$_2$ZrCl$_2$/MAO (**67**) exhibit quasi-living behavior for ethylene-norbornene copolymerizations (Figure 1.21).

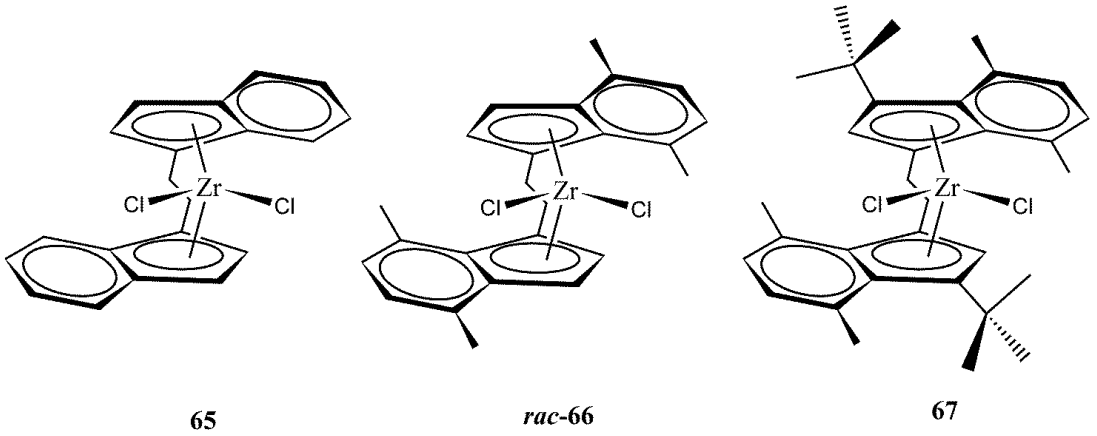


**65** ***rac*-66** **67**

**Figure 1.21.** *Zirconocenes complexes for living ethylene-norbornene polymerization.*

At 30 °C, **65**/MAO exhibits a constant rate during the first hour of polymerization, while **66**/MAO and **67**/MAO exhibited a decrease in polymerization rate. Narrow molecular weight distributions were obtained at short reaction times (**65**/MAO, t = 10 min, $M_w/M_n$ = 1.24) but broadened quickly (t = 20 min, $M_w/M_n$ = 1.50).For **65**/MAO and **66**/MAO, the $M_n$ of the copolymer was shown to increase during the first 45 minutes and then levels off; for catalyst **67**/MAO the increase in $M_n$ lasted 30 minutes. Finally, the molecular weight and norbornene content of the resultant copolymers were shown to decrease with increasing steric demand of the ligand framework.

### 1.5.5.1 Titanium catalysts

Fujita [70] reported first the synthesis of ethylene-norbornene copolymers with bis(pyrrolide-imine)titanium complexes, which are reported in Figure 1.22, in 2000.

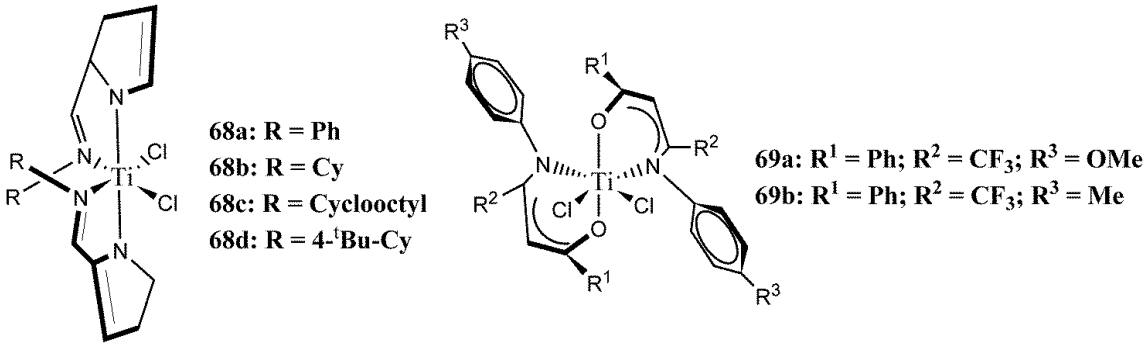


**Figure 1.22.** *Bis(pyrrolide-imine) and bis(enaminoketonato) titanium catalysts.*

Upon activation with MAO or $[Ph_3C][B(C_6F_5)_4]/Al(i\text{Bu})_3$ at 25 °C, compounds **68a** and **68b** exhibited extremely high activities for ethylene polymerization, and produced high molecular weights ($M_w$ = 75.000-4.739.000 g/mol). Encouraged by these results, Fujita turned his attention to the copolymerization of ethylene and norbornene [71]. In fact, in the presence of ethylene and norbornene, **68** furnished poly(E-*alt*-N) with narrow molecular weight distributions and high molecular weights (**68a**: $M_w/M_n$ = 1.10, $M_n$ = 127.000 g/mol; **68b**: $M_w/M_n$ = 1.16, $M_n$ = 521.000 g/mol; **68c**: $M_w/M_n$ = 1.23, $M_n$ = 600.000 g/mol; **68d**: $M_w/M_n$ = 1.24, $M_n$ = 417.000 g/mol). The copolymers were found to contain 95.4 % perfectly alternated N-E units. Copolymerizations by **68a-d** showed a linear increase of $M_n$ with time over the course of 20 minutes. It is worth noting that under the conditions employed, catalysts **68a-d** are living for ethylene homopolymerization for only very short time (30 seconds) and inactive for norbornene homopolymerization.

Copolymerization of ethylene and norbornene by catalysts **56-60** (Figure 1.14) was also shown to possess some living characteristics [43]. The polymerization conducted at 25 °C gave narrow molecular weight distributions ($M_w/M_n$ = 1.07-1.54) with $M_n$ around 150.000-580.000 g/mol, while the norbornene content ranged from 35.3 to 55.4 %. Moreover, Li and coworkers [72,73] discussed the effects of ligand modifications on the copolymerization behavior, passing from catalyst **56** to **69**: by replacing the *N*-phenyl group with a *p*-anisole (**69a**) or *p*-tolyl (**69b**), a marked increase in ethylene homopolymerization was observed with a parallel broadening of molecular weight distribution. So, while the living character of ethylene polymerization was lost, **69b** showed a quasi-living behavior in ethylene-norbornene copolymerization. At 25 °C, this system produced P(E-*co*-N) with narrow polydispersity ($M_w/M_n$ = 1.18-1.31). The copolymers possessed high molecular weights ($M_n$ 200.000-570.000 g/mol) with

norbornene content ranging from 44.7 to 47.8 mol %. The polymerization displayed a linear increase of $M_n$ with time, from 5 to 20 min.

### 1.5.5.2 Palladium catalysts

Kaminsky applied a combinatorial screening approach to identify catalysts for the copolymerization of ethylene with norbornene [74].

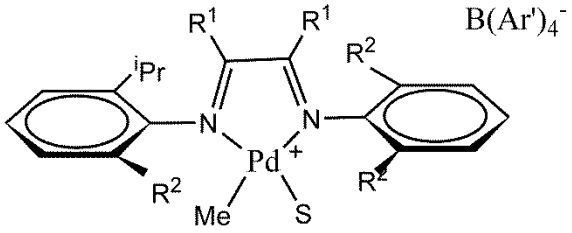


**70a: $R^1$ = H, $R^2$ = Me, S = $CH_3CN$**
**70b: $R^1$ = Me, $R^2$ = *i*Pr, S = $CH_3CN$**

**Figure 1.23.** *Palladium catalysts for living ethylene-norbornene copolymerization.*

Promising leads were identified in complexes **70a** and **70b** (Figure 1.23). Catalyst **70b** generated copolymers with 9-40 mol % norbornene incorporation and $M_w/M_n$ as low as 1.5. Catalyst **87a** is sterically less congested and so able to incorporate up to 62 % norbornene, with $M_w/M_n$ = 1.4, and some block formation was observed. This catalyst demonstrates a dramatic comonomer effect, with the polymerization rate increasing sharply with increasing norbornene concentration in the feed up to 10%. At this level, the activity is competitive with metallocene catalysts Above this, productivity drops off, and activity for norbornene homopolymerization is negligible. This effect was not observed for **70b**, which was most active for ethylene homopolymerization. Although not rigorously shown to be living, these systems produced copolymers with molecular weight distributions less than 2 at 30 °C.

## 1.5.6 Block copolymers

The importance of living polymerization catalysts is considerably dependent on their ability to form block copolymers [75], which is typically achieved via sequential monomer addition, from common commercial monomers, such as ethylene and propylene, or ethylene ad norbornene, since these materials have applications as compatibilizers and elastomers.

Physical blends, or random copolymers often give rise to materials whose properties are intermediate between those of the respective homopolymers. Block copolymers, on the other hand, often furnish materials whose mechanical properties are superior to the sum of their parts: this unique behavior is due to microphase separation of the different segments of the block copolymer into discrete domains which gave rise to otherwise unattainable morphologies.

A sought goal in the field of olefin polymerization is the synthesis of block copolymers containing *i*PP domains: they are envisioned to possess material properties of great industrial interest. For example, they may serve as compatibilizers in blends containing *iPP* homopolymers [75,76].

A particularly desirable type of block copolymer structures is that with "hard" or semicrystalline end blocks (e.g. PE, *i*PP, *s*PP) and amorphous mid blocks (e.g. *a*PP, poly(E-*co*-P), LLPE); triblock copolymers of this type have been shown to behave as thermoplastic elastomers [77].

Although individual catalyst systems have been reported which achieve some characteristics of a living polymerization, the preparation of olefin block copolymers having both "hard" (semicrystalline or high glass transition temperature) and "soft" (amorphous and low glass transition temperature) segments remains a major challenge in the field of polymerization catalysis.

### 1.5.6.1 Polyethylene containing block copolymers

Bis(phenoxyimine) titanium complexes can provide highly syndiotactic PP and poly(E-*co*-P) blocks have also been synthesized.

For example, using **8**/MAO [78] a PE-*block*-poly(E-*co*-P) and a triblock PE-*block*-poly(E-*co*-P)-*block*-PE were synthesized. The molecular weight was high while molecular weight distributions remained low, in both cases.

With bis(indolide-imine)titanium complex **54**/MAO [79,80] Fujita was able to prepare PE-*block*-poly(E-*co*-P). The PE block exhibited a narrow polydispersity ($M_w/M_n$ = 1.05) with $M_n$ = 15.200 g/mol. The low PDI was maintained also for the diblock copolymer with an increase in molecular weight to $M_n$ = 31400 g/mol. TEM visualization of the material revealed microphase separation of PE and poly(E-*co*-P) domains, which were dispersed throughout the sample: this is in contrast with the case of PE-poly(PE-*co*-P) blend, which possessed well defined PE and lamellas of P(E-*co*-P) with lengths greater than 100 nm.

### 1.5.6.2 Block copolymers of ethylene with norbornene

After the alternating copolymerization of ethylene and norbornene using bis(pyrrolideimine)titanium catalyst, Fujita was able to utilize these catalysts to prepare block copolymers containing poly(E-*co*-N) and PE segments with varyiong degrees of norbornene incorporation [81].

Block copolymers of the type poly(E-*co*-N)x-*block*-poly*(E-co*-N)$_y$ were prepared by initiating the polymerization in a toluene solution saturated with ethylene and containing the desired amount of norbornene, allowing the polymerization to proceed for a proper time. After the first block had been formed, additional norbornene was added while maintaining the ethylene feed. The blocky nature was evidenced by the observation of multiple thermal transitions in the DSC thermograms. For example (Scheme 1.2), a block copolymer with 7.6 % norbornene incorporation in the first block and 27.4 % norbornene in the second one, exhibited a $T_m$ = 88 °C relative to the crystalline first block, and a $T_g$ = 116 °C for the second block. Increasing norbornene incorporation (> 19.5 mol % first block, >30.1 mol % second block) two second order thermal transitions were observed, that is one for each block.

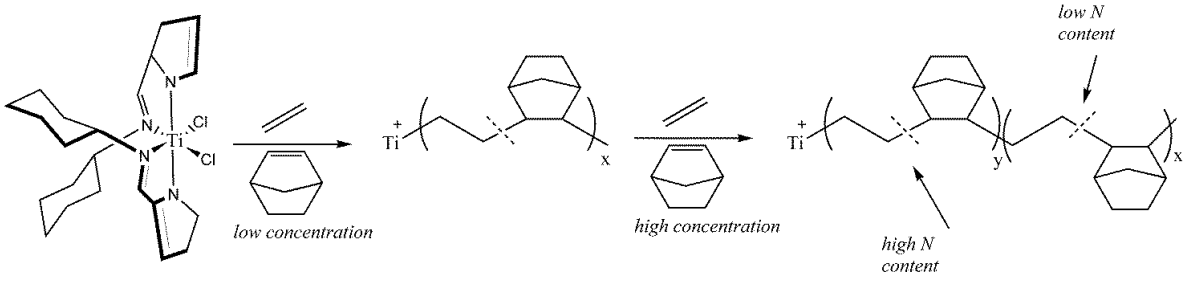


**Scheme 1.3.** *Synthesis of ethylene/norbornene block copolymers.*

PE-*block*-poly(E-*co*-N) was prepared with **68b**/MAO under continuous feed of ethylene diluted with dinitrogen at 25 °C for 10 s to furnish a PE segment with $M_n$ = 119.000 g/mol and $M_w/M_n$ = 1.34. The $N_2$ flow was discontinued and 10 g of norbornene was added resulting in the formation of the copolymer block. The final polymer exhibited a narrow polydispersity ($M_w/M_n$ = 1.56) and $M_n$ = 414.000 g/mol with a norbornene content of 31.5 mol %. TEM images reveal significant inhomogeneities due to phase separation.

Copolymers of ethylene and norbornene have also been synthesized by using **9**/MAO [82]: a high molecular weight, low PDIs poly(E-*co*-N) sample was prepared ($M_n$ = 238.000 g/mol, $M_w/M_n$ = 1.05). The copolymer contained 62 mol % ethylene and a $T_g$ of

86.5 °C. Moreover, **9**/MAO was used to synthesize a high molecular weight poly(E-*co*-P)-*block*-poly(E-*co*-N) sample ($M_n$ = 576.000 g/mol, $M_w/M_n$ = 1.13).

Li and coworkers prepared block copolymers of ethylene and norbornene using various bis(enaminoketonato)titanium catalysts [83], by sequential monomer addition: to an ethylene saturated solution at 25 °C, **56**/MAO was added and ethylene polymerization was allowed to proceed for 5 min after which 5 g of norbornene was added and reaction proceeded further 5 min. The resultant PE block possessed narrow molecular weight distribution ($M_w/M_n$ = 1.3) with $M_n$ = 96.999 g/mol; the diblock copolymer retained a narrow polydispersity ($M_w/M_n$ = 1.38) and increased in molecular weight ($M_n$ = 143.000 g/mol), with a norbornene content of 11.1 mol %. PE-*block*-poly(E-*co*-CP) was prepared in an identical manner [84].

Catalyst **3** was proved to be suitable for polypropylene as well as poly(E-*co*-N) living polymerization. In 2006, Shiono was able to prove that **3**/MAO could also copolymerize propylene and norbornene in a living fashion, giving random and block copolymers [85]. A poly(P-*co*-N) sample was synthesized having $M_n$ = 82000 g/mol and $M_w/M_n$ = 1.12. The copolymer exhibited a very high $T_g$ value of 252 °C. After that, three *s*PP-*block*-poly(E-*co*-N) diblock copolymers were synthesized, having similar molecular weights, around 20.000 g/mol, and narrow PDIs ($M_w/M_n$ = 1.21-1.32). It is worth noting that the best results for living polymerization of ethylene with norbornene, and with block copolymers, in terms of molecular weight distributions, yields, activities are only achievable at low temperature, with a maximum of 25-30 °C.

## 1.6 Motivation

As seen before, titanium$^{(IV)}$ complexes with bidentate *N*,*O*-donor ligands have attracted considerable attention as catalysts for olefin polymerization, especially with regards to their potential to induce living polymerization [86].

In particular, complex **64b** was found to polymerize ethylene in a living fashion with unprecedented molar masses control and thermal stability up to 75 °C [44,45].

On the other hand, despite the importance of ethylene-norbornene copolymers in various fields owing to their extraordinary material properties [61-64], there are only few examples of catalysts that give living E-*co*-N copolymerization [83,84], and only at room temperature: the synthesis of polyolefins at high temperature with truly narrow distribution remains a challenge.

Therefore, the first part of this Thesis will be dedicated to the evaluation of complex **64b** upon activation with MAO for the copolymerization of ethylene with norbornene, in a wide range of temperatures from 25 till 90 °C, and at different [N]/[E] ratios, proving catalysts' living features and the subsequent synthesis of block copolymers. All the synthesized copolymers and block copolymers will be completely characterized by means of DSC, TGA, GPC, and NMR.

Moreover, the presence of fluoroaryl substituents on the aryl moieties was found to be compulsory to trigger the living polymerization mechanism. Their role could apparently consist in suppression of chain termination process, thus allowing consecutive enchainment without termination. The possible mechanism is really intriguing and still remains under debate [87-90]. To date, there are no studies available regarding the mechanism of living ethylene-norbornene copolymerization reaction using complex **64b**/MAO. The second part of this Thesis will therefore regard a multinuclear NMR spectroscopic study, trying to define the active species involved in the living copolymerization reaction, and in particular the role of fluorine substituents will be discussed.

## 1.7 References


1. Current economic data are available at www.plasticeurope.org
2. Ziegler K, Holzkamp E, Breil H, Martin H *Angew. Chem.* **1955**, *67*, 426.
3. Natta G, Pino P, Corradini P, Danusso F, Mantica E, Mazzanti G, Moraglio G *J. Am. Chem. Soc.* **1955**, *77*, 1708.
4. Szwarc M *J Polym Sci Part A: Polym Chem* **1998**, *36*, 9.
5. Quirk RP, Lee B *Polym Int* **1992**, *27*, 359.
6. Zambelli A, Natta G, Pasquon I, Signorin R *J Polym Sci Part C: Polym Symp* **1967**, *99*, 2485.
7. Doi Y, Ueki S, Keii T *Macromolecules* **1979**, *12*, 814; Doy Y, Ueki S, Keii T *Makromol Chem Macromol Chem Phys* **1979**, *180*, 1359.
8. Sassmannshausen J, Bochmann M, Rosch J, Lilge D *J Organomet Chem* **1997**, *548*, 23.
9. Fukui Y, Murata M, Soga K, *Macromol Rapid Commun* **1999**, *20*, 637.
10. Yasumoto T, Yamagata T, Mashima K *Organometallics* **2005**, *24*, 3375.
11. Cai ZG, Ikeda T, Akita M, Shiono T *Macromolecules* **2005**, *38*, 8135.

12. Nishii K, Ikeda T, Akita M, Shiono T *J Mol Cat A: Chem* **2005**, *231*, 241.
13. Sakuma A, Weiser M.-S, Fujita T *Polymer Journal* **2007**, *39*, 193.
14. Matsui S, Tohi Y, Mitani M, Saito J, Makio H, Tanaka H, Nitabaru M, Nakano T, Fujita T *Chem Lett* **1999**, 1065; b) Matsui S, Mitani M, Saito J, Tohi Y, Makio H, Tanaka H, Fujita T *Chem Lett* **1999**, 1263; c) Matsui M, Saito J, Matsukawa N, Tanaka H, Nakano T, Fujita T *Chem Lett* **2000**, 554.
15. a) Matsui S, Mitani M, Saito J, Tohi Y, Makio H, Matsukawa N, Takagi Y, Tsuru K, Nitabaru M, Nakano T, Tanaka H, Kashiwa N, Fujita T *J Am Chem Soc* **2001**, *123*, 6847; b) Ishii S, Saito J, Mitani M, Mohri J, Matsukawa N, Tohi Y, Matsui S, Kashiwa N, Fujita T *J Mol Cat A Chem* **2002**, *179*, 11; c) Ishii S, Saito J, Matsuura S, Suzuki Y, Furuyama R, Mitani M, Nakano T, Kashiwa N, Fujita T *Macromol Rapid Commun* **2002**, *23*, 693; d) Furuyama R, Saito J, Ishii S, Mitani M, Matsui S, Tohi Y, Makio H, Matsukawa N, Tanaka H, Fujita T *J Mol Cat A Chem* **2003**, *31*, 200; e) Nakayama Y, Bando H, Sonobe Y, Kaneko H, Kashiwa N, Fujita T *J Catal* 2003, *215*, 171.
16. Tian J, Coates GW *Angew Chem Int Ed* **2000**, *39*, 3626.
17. Tian J, Hustad PD, Coates GW *J Am. Chem. Soc.* **2001**, *123*, 5134.
18. Saito J, Mitani M, Mohri J, Ishii S, Yoshida Y, Matsugi T; Kojoh S.-I, Kashiwa N, Fujita T *Chem Lett* **2001**, 576.
19. Nakayama Y, Saito J, Bando H, Fujita T *Macromol Chem Phys* **2005**, *206*, 1847.
20. Mason AF, Coates GW *J Am Chem Soc* **2005**, *126*, 10798.
21. Domski GJ, Rose JM, Coates GW, Bolig AD, Brookhart M *Prog Polym Sci* **2007**, *32*, 30.
22. Mason AF, Coates GW *J Am Chem Soc* **2004**, *126*, 16326.
23. Reinartz S, Mason AF, Lobkovsky EB, Coates GW *Organometallics* **2003**, *22*, 2542.
24. Ittel SD, Johnson LK, Brookhart M *Chem Rev* **2000**, *100*, 1169.
25. Jeske G, Lauke H, Mauermann H, Swpston PN, Schumann H, Marks TJ *J Am Chem Soc* **1985**, *107*, 8091.
26. Bambirra S, van Leusen D, Meetsma A, Hessen B, Teuben JH *Chem Commun* **2003**, *27*, 522.
27. Wang W, Nomura K *Macromolecules* **2005**, *38*, 5905.

28. Mashima K, Fujikawa S, Urata H, Tanaka E, Nakamura A *J Am Chem Soc* **1993**, *115*, 10990.
29. Mashima K, Fujikawa S, Urata H, Tanaka E, Nakamura A *J. Chem. Soc. Chem. Commun.* **1994**, *32*,1623.
30. MacAdams LA, Buffone GP, Incarvito CD, Rheingold AL, Theopold KH *J Am Chem Soc* **2005**, *127*, 1082.
31. Brookhart M, DeSimone JM, Grant BE, Tanner MJ *Macromolecules* **1995**, *28*, 5378.
32. Gottfried AC, Brookhart M *Macromolecules* **2001**, *34*, 1140.
33. Gottfried AC, Brookhart M *Macromolecules* **2003**, *36*, 3085.
34. Camacho DH, Salo EV, Ziller JW, Guan ZB *Angew Chem Int Ed* **2004**, *43*,1821.
35. Hicks FA, Jenkins JC, Brookhart M *Organometallics* **2003**, *22*, 3533.
36. Diamanti SJ, Ghosh P, Shimizu F, Bazan GC *Macromolecules* **2003**, *36*, 9731.
37. Saito J, Mitani M,; Mohri J, Yoshida Y, Matsui S, Ishii S, Kojoh SI, Kashiwa N, Fujita T *Angew Chem Int Ed* **2001**, *40*, 2918.
38. Furuyama R, Saito J, Ishii S, Makio H, Mitani M, Tanaka H, Fujita T *J Organomet Chem* **2005**, *690*, 4398.
39. a) Makio H, Kashiwa N, Fujita T *Adv Synth Catal* **2002**, *344*, 477; b) Mitani M, Mohri J, Yoshida Y, Saito J, Ishii S, Tsuru K, Matsui S, Furuyama R, Nakano T, Tanaka H, Kojoh S.-I, Matsugi T, Kashiwa N, Fujita T *J Am Chem Soc* **2002**, *124*, 3327.
40. Mitani M, Mohri J, Furuyama R, Ishii S, Fujita T *Chem Lett* **2003**, *32*, 238.
41. Furuyama R, Saito J, Ishii S, Makio H, Mitani M, Tanaka H, Fujita T *J Organomet Chem* **2005**, *690*, 4398.
42. a) Matsugi T, Matsui S, Kojoh S, Takagi Y, Inoue Y, Fujita T, Kashiwa N *Chem Lett* **2001**, *158*, 566; b) Matsugi T, Matsui S, Kojoh S, Takagi Y, Inoue Y, Nakano T, Fujita T, Kashiwa N *Macromolecules* **2002**, *35*, 4880; c) Yoshida, Y, Matsui S, Fujita T *J Organomet Chem* **2005**, *690*, 4382.
43. Li X.-F, Dai K, Ye, W.-P, Pan L, Li Y.-S. *Organometallics* **2004**, *23*, 1223.
44. Yu S.-M., Mecking S *J Am Chem Soc* 2008, 130, 13204
45. Yu S.-M., Tritschler U, Gottker-Schnetmann I, Mecking S Dalton Trans 2010, 39, 4612.
46. Sargusa T, Tsujino T, Furukawa J *Makromol Chem* **1964**, *78*, 231.

47. (a) Kaminsky W, Bark A, Arndt M *Makromol Chem Macromol Symp* **1991**, *47*, 83; (b) Kaminsky W, Noll A *Polym Bull* **1993**, *31*, 175; (c) Kaminsky W, Arndt W *Adv Polym Sci* **1997**, *127*, 143; (d) Kaminsky W, Arndt-Rosenau M in: Scheirs J, Kaminsky W (Eds.), Metallocene-based Polyolefins, Wiley, Chichester, **2000**, p.89 (e) Kaminsky W, Beulich I, Arndt M *Macromol Symp* **2001**, *173*, 211.
48. US 3074918 (**1960**), Du Pont, inv.: Eleuterio HS.
49. Herisson J.-L, Chauvin Y *Makromol Chem* **1970**, *141*, 161.
50. Reif L., Hocker H *Makromol Chem Rapid Commun* **1981**, *2*, 183.
51. (a) Thorn-Csanyi E, Ruhland K *Macromol Chem Phys* **1999**, *200*, 1662; (b) Thorn-Csanyi E, Ruhland K *Macromol Chem Phys* **1999**, *200*, 2245; (c) Thorn-Csanyi E, Ruhland K *Macromol Chem Phys* **1999**, *200*, 2606; (d) Thorn-Csanyi E, Ruhland K *Macromol Symp* **2000**, *153*, 145.
52. Schrock RR, DePue RT, Feldmann J, Schaverien CJ, Dewan JC, Liu AH *J Am Chem Soc*, **1988**, *110*, 1423.
53. France MB, Paciello RA, Grubbs RH *Macromolecules* **1993**, *26*, 4742.
54. Dall'Asta G, Motroni D *Eur Polym J* **1971**, *7*, 707.
55. Benson SW, Cruickshank FR, Golden DM, Haugen GR, O'Neal HE, Rodgers AS, Shaw R, Walsh R *Chem Rev* **1969**, *69*, 279.
56. Seehof N, Mehler C, Breunig S, Risse W *J Mol Catal* **1992**, *76*, 219.
57. Mecking S *Coord Chem Rev* **2000**, *203*, 325.
58. Goodall L, McIntosh LH III, Rhodes LF *Makromol Chem Macromol Symp* **1995**, *89*, 421.
59. Mehler C, Risse W *Macromolecules* **1992**, *25*, 4226.
60. Breunig S, Risse W *Makromol Chem* **1992**, *193*, 2915.
61. www.topas.it
62. Brekner MJ, Osan F, Rohrmann J, Antberg M (**1994**) Process for the preparation of chemically homogeneous cycloolefin copolymers, US Patent 5,324,801, 199.
63. Modern Plastics (**1995**) 72:137
64. Boggioni L, Tritto I *Adv Polym Sci* **2013**, *258*, 117.
65. Hasan T, Shiono T, Ikeda T *Macromol Symp* **2004** , *213*, 123.
66. Hasan T, Ikeda T, Shiono T *Macromolecules* **2004**, *37*, 8503.
67. Hasan T, Ikeda T, Shiono T *Macromolecules* **2005**, *38*, 1071.

68. Jansen JC, Mendichi R, Locatelli P, Tritto I *Macromol Rapid Commun* **2001**, *22*, 1394.
69. Jansen JC, Mendichi R, Sacchi MC, Tritto I *Macromol Chem Phys* **2003**, *204*, 522.
70. Yoshida Y, Matsui S, Takagi Y, Mitani M, Nitabaru M, Nakano T, Fujita T *Chem Lett* **2000**, 1270.
71. a) YoshidaY, Saito J, Mitani M, Takagi Y, Matsui S, Ishii S, Fujita T *Chem Commun* **2002**, 1298; b) Yoshida Y, Matsui S, Takagi Y, Mitani M, Saito J, Ishii S, Fujita T in: Anpo M, Onaka M, Yamashita H Editors, Science and Technology in Catalysis **2002**, p. 521; c) Yoshida Y, Mohri J, Ishii S, Mitani M, Saito J, Matsui S, Fujita T *J Am Chem Soc* **2004**, *126*, 12023.
72. Tang LM, Hu T, Bo YJ, Li Y.-S *J Organomet Chem* **2005**, *690*, 3125.
73. Tang LM, Duahn YQ, Pan L, Li Y.-S *J Polym Sci Part A: Polym Chem* **2005**, *43*, 1681.
74. Kiesewetter J, Kaminski W *Chem Eur J* **2003**, *9*, 1750.
75. a) Ruzette AV, Leibler L *Nat Mater* **2005**, *4*, 19; b) Bates FS *Science* **1991**, *251*, 898.
76. Karian H. G. in Handbook of polypropylene and polypropylene composites. New York: Marcel Dekker Inc, (**2003**).
77. a) Mallin DT, Rausch MD, Lin YG, Dong SZ, Chien JCW *J Am Chem Soc* **1990**, *112*, 2030; b) Coates GW, Waymouth RM *Science* **1995**, *267*, 217; c) Chien JCW, Iwamoto Y, Rausch MD, Wedler W, Winter HH *Macromolecules* **1997**, *30*, 3447; d) Lieber S, Brintzinger HH *Macromolecules* **2000**, *33*, 9192; e) Harney MB, Zhang YH, Sita, LR *Angew Chem Int Ed* **2006**, *45*, 2400.
78. Mitani M, Mohri J, Yoshida Y, Saito J, Ishii S, Fujita T *J Am Chem Soc* **2002**, *124*, 3327.
79. Matsugi T, Matsui S, Kojoh S, Takagi Y, Inoue Y, Nakano T *Macromolecules* **2002**, *35*, 4880.
80. Matsugi T, Matsui S, Kojoh S, Takagi Y, Inoue Y, Nakano T in: Anpo M, Onaka M, Yamashita H, Editors. Science and technology in Catalysis 2002 (**2003**), p. 523.
81. Yoshida Y, Mohri J, Ishii S, Mitani M, Saito J, Matsui S *J Am Chem Soc* **2004**, *126*, 12023.
82. Yoon J, Mathers RT, Coates GW, Thomas EL *Macromolecules* **2006**, *39*, 1913.
83. Li XF, Dai K, Ye WP, Pan L, Li Y.-S *Organometallics* **2004**, *23*, 1223.

84. Tang LM, Duan YQ, Pan L, Li Y.-S *J Polym Sci Part A: Polym Chem* **2005**, *43*, 1681.

85. Cai ZG, Nakayama Y, Shiono T *Macromolecules* **2006**, *39*, 2031.

86. a) Makio H, Terao H, Iwashita A, Fujita T *Chem Rev* **2011**, *111*, 2363; b) Makio H, Kashiwa N, Fujita T *Adv Synth Catal* **2002**, *344*, 477; c) Saito J, Mitani M, Mohri J, Ishii S, Yoshida Y, Matsugi T, Kojoh S, Kashiwa N, Fujita T *Chem Lett* **2001**, *30*, 573; d) Mitani M, Nakano T, Fujita T *Chem Eur J* **2003**, *9*, 2396; e) Furuyama R, Mitani M, Mohri J, Mori R, Tanaka H, Fujita T Macromolecules **2005**, *38*, 1546; f) Makio H, Fujita T *Acc Chem Res* **2009**, *42*, 1532.

87. a) Kui SCF, Zhu N, Chan MCW *Angew Chem Int Ed* **2003**, *42*, 1627; b) Chan MCW, Kui SCF, Cole JM, McIntyre GJ, Matsui S, Zhu N, Tam KH *Chem Eur J* **2006**, *12*, 2607; c) Chan MCW *Chem Asian J* **2008**, *3*,18; d) So LC, Liu CC, Chan MCW, Lo JCY, Sze KH, Zhu M *Chem Eur J* **2012**, *18*, 566; e) Iwashita A, Chan MCW, Makio H, Fujita T *Catal Sci Technol* **2014**, *4*, 599.

88. Talarico G, Busico V, Cavallo L *Organometallics* **2004**, *23*, 5989.

89. Villani V, Giammmarino G *Macromol Theory Simul* **2011**, *20*, 174.

90. a) Bryliakov KP, Talsi EP, Moller HM, Baier MC, Mecking S *Organometallics* **2010**, *29*, 4428; b) Moller HM, Baier MC, Mecking S, Talsi EP, Bryliakov KP *Chem Eur J* **2012**, *18*, 848.

# 2 Results and discussion 1:

## Living ethylene-norbornene copolymerization and block copolymers synthesis

### 2.1 Introduction

In the family of complexes with N,O-chelating ligands, phenoxyimine Ti systems with *o*-fluorine (*o*-F) substitution of the N-aryl moiety were reported as highly active versatile catalysts for the synthesis of narrowly distributed polyolefins.

A family of titanium complexes with enaminoketonato ligands with tuned electronic density and encumbrance at the metal center was also reported by Li [1].

These systems readily afford PE and P(E-*co*-N) with fairly narrow $M_w/M_n$ at room temperature. Afterward, the analogous titanium complex [Ti($\kappa_2$-N,O-{2,6-$F_2C_6H_3N$=C(Me)C(H)C($CF_3$)O})$_2Cl_2$] upon activation with MAO has been proved to be a highly active versatile catalyst for the living synthesis of polyolefins with unprecedented molar mass control and thermal robustness, even at temperatures as high as 75 °C [2]. This unique feature was attributed to the stabilization of Ti center toward β-H elimination and chain transfer, imparted by the noncovalent interaction with *o*-F substituents on aryl moiety 3.

Here, the E-*co*-N copolymerization reaction with complex **1** activated with dried-MAO (*d*-MAO) was investigated in a wide range of temperatures between 25 and 90 °C, under an atmospheric pressure of ethylene in toluene, as represented in Scheme 2.1.

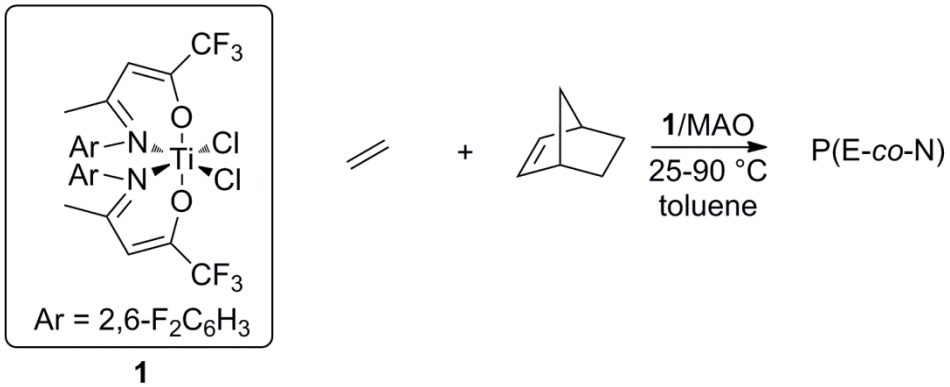


**Scheme 2.1** *Copolymerization reaction of ethylene with norbornene using titanium complex 1 upon activation with d-MAO.*

## 2.2 Living ethylene-*co*-norbornene copolymerization

Norbornene content and copolymer microstructure were determined from the analysis of $^{13}C$ NMR spectra; glass transition temperatures and molar masses were estimated by DSC and SEC measurements, respectively. Selected results are summarized in Table 2.1.

**Table 2.1. Selected results and conditions for copolymerization of ethylene with norbornene by catalyst 1/*d*-MAO**

| Run[a] | *T* °C | *t* min | *V* mL | [N]/[E] | Yield mg | *A*[b] | ($T_m$)[c] $T_g$ °C | N[d] mol % | $M_n$[e] kg mol$^{-1}$ | $M_w/M_n$[e] |
|---|---|---|---|---|---|---|---|---|---|---|
| **1**[f] | 50 | 5 | 250 | - | 163 | 1954 | (135) | - | 111 | 1.37 |
| **2** | 50 | 5 | 125 | 1 | 266 | 6389 | 107 | 42.0 | 464 | 1.15 |
| **3** | 50 | 15 | 50 | 1.5 | 472 | 3777 | 99 | 39.0 | 731 | 1.29 |
| **4** | 50 | 15 | 50 | 3 | 681 | 5448 | 118 | 44.2 | 958 | 1.32 |
| **5** | 50 | 15 | 50 | 6 | 630 | 5039 | 121 | 45.2 | 990 | 1.27 |
| **6** | 25 | 5 | 125 | 2 | 234 | 5624 | 112 | - | 411 | 1.14 |
| **7** | 50 | 5 | 125 | 2 | 255 | 6136 | 104 | 41.2 | 445 | 1.15 |
| **8** | 75 | 2 | 125 | 2 | 113 | 6766 | 119 | 42.6 | 209 | 1.08 |
| **9** | 75 | 5 | 125 | 2 | 218 | 5220 | 118 | 43.0 | 325 | 1.24 |
| **10** | 90 | 5 | 125 | 2 | 184 | 4405 | 123 | 43.7 | 295 | 1.24 |
| **11** | 50 | 2 | 125 | 2 | 109 | 6554 | 107 | - | 194 | 1.12 |
| **12** | 50 | 3.5 | 125 | 2 | 181 | 6209 | 106 | 36.6 | 318 | 1.14 |
| **7** | 50 | 5 | 125 | 2 | 255 | 6136 | 105 | 41.2 | 445 | 1.15 |
| **13** | 50 | 10 | 125 | 2 | 574 | 6885 | 117 | 42.9 | 865 | 1.22 |

[a] ***1*** *= 0.5 μmol; MAO: Al/Ti = 2000/1; $V_{toluene}$ =125 mL; T = 50 °C; p(E)= 1.01 bar*
[b] *Activity in kg polymer ·mol Ti$^{-1}$ h$^{-1}$*
[c] *Determined by DSC, second heating scan*
[d] *Determined by $^{13}C$ NMR in $C_2D_2Cl_4$ at 103 °C with HMDS as reference*
[e] *Determined by SEC in o-$C_6H_4Cl_2$ with standard PS calibration.*
[f] ***1*** *= 1 μmol; MAO: Al/Ti = 2,000/1; $V_{toluene}$ = 250 mL; T = 50 °C; p(E) =1.01 bar*

Run **1** confirms that **1**/*d*-MAO is a highly active catalyst for ethylene polymerization, affording high-molecular-weight ($M_n$ = 1.1 · $10^5$ g mol$^{-1}$) linear PE with living characteristics at 50 °C, that is, narrow molecular weight distribution ($M_w/M_n$ =

1.37) after 5 min of polymerization. Polyethylenes were prepared under similar conditions in the group of Mecking; they found narrower $M_w/M_n$ distributions probably due to differences in SEC instrumentation and calibration (PS standards *vs* PE standards) 2.

When used in E-*co*-N copolymerization at [N]/[E] = 1, the catalytic system, for 5 min polymerization time, yielded higher activity and molecular weight E-*co*-N copolymer with narrower distribution ($M_w/M_n$ = 1.15, run 2).

The E-*co*-N copolymerization was explored at 50 °C at different [N]/[E] ratios: the increase in molar masses with [N]/[E] ratio in feed is more evident in copolymerization at higher [N]/[E] values; in fact passing from [N]/[E] ratios of 1.5 to [N]/[E] ratios of 3 there is an increase in the molecular weight, passing from 731 up to 958 kg mol$^{-1}$.

The effect of temperature on the living characteristics of these copolymerizations was studied at [N]/[E] ratio of 2 in the range of temperatures between 25 and 90 °C. An increase in yield and molar masses is observed when raising the temperature from 25 to 50 °C (runs 6 and 7), whereas both yields and molar masses decrease with a further rise of the temperature (runs 9 and 10), as depicted in Figure 2.1.

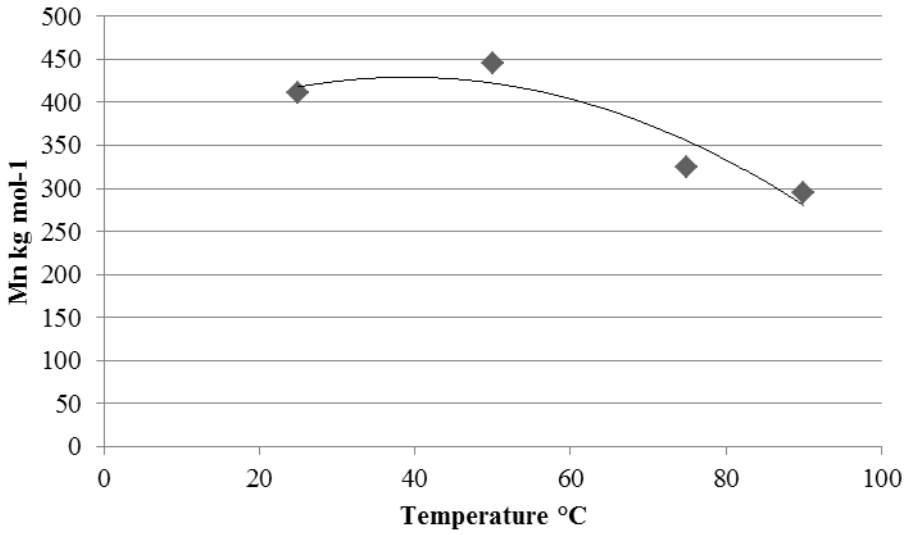


**Figure 2.1** *Molecular weight evolution with temperature for entries 6, 7, 9, and 10.*

Moreover, this is accompanied by a slight broadening of the molar mass distributions.

The increase in propagation rate obtained by increasing the temperature and the living nature of the catalytic system account for the increase in activity and molar mass up to 50 °C. However, it seems that the robustness of this catalytic system at high temperature,

proven in ethylene polymerization 2, decreases in the presence of norbornene. It is worth noting that at 75 °C, at reaction time as low as 2 min, molar mass distribution of E-*co*-N copolymers is still very narrow ($M_w/M_n$ = 1.08, run 8). Since the best yields, activities and molecular weights' results were obtained at 50 °C, the living nature of the copolymerization was fully demonstrated through kinetic studies at 50 °C and at [N]/[E] = 2. SEC analysis of the copolymers showed that molecular masses shifted to higher values according to the polymerization time (Figure 2.2).

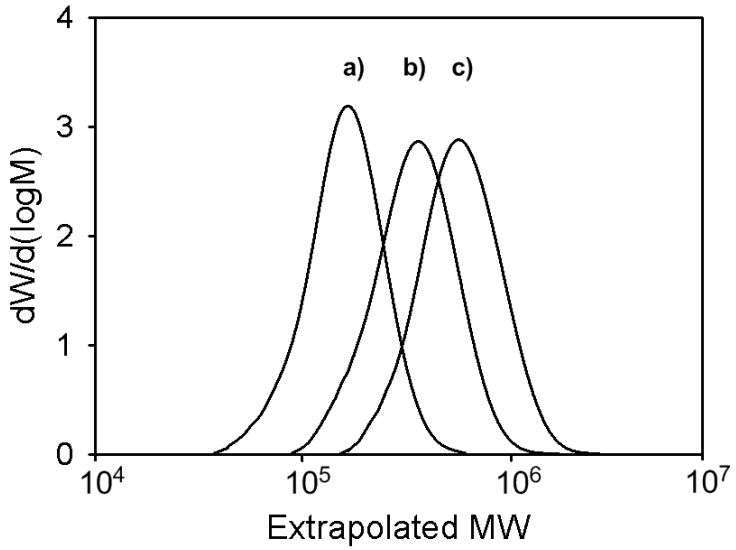


**Figure 2.2.** *SEC profiles of P(E-co-N) obtained by 1/d-MAO at 50 °C and [N]/[E] = 2 at different reaction times. (a) run 11, (b) run 12; (c) run 7 of Table 2.1.*

The increase in molar masses with polymerization time is clearly shown in Figure 2.3, where $M_n$ and $M_w/M_n$ values are plotted against the time, which demonstrates a good linear relationship while keeping narrow $M_w/M_n$. These results testified that the copolymerization of ethylene and norbornene with complex **1** upon *d*-MAO activation proceeds in a living manner.

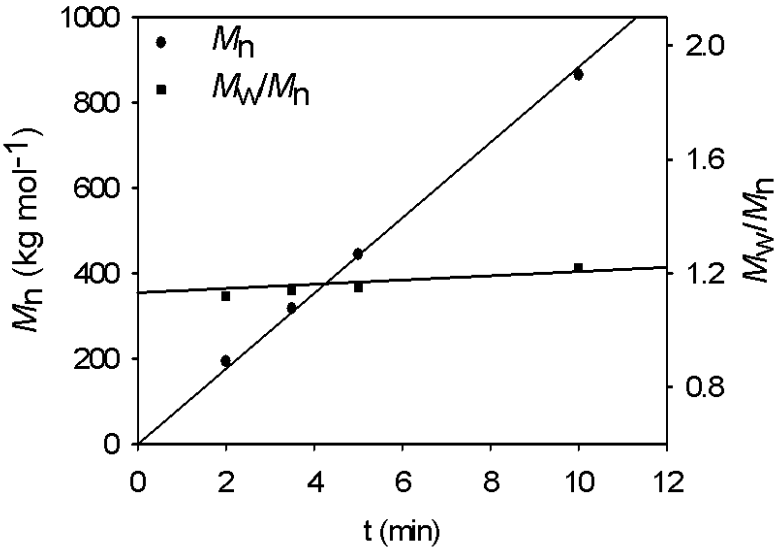


**Figure 2.3.** *Plots of Mn and Mw/Mn vs. time for the copolymerization of ethylene with norbornene at 50 °C and [N]/[E] = 2 with* ***1****/d-MAO (runs 11, 12, 7, 13, Table 2.1).*

The thermal properties, measured by DSC, reveal that the synthesized copolymers are amorphous with glass transition temperatures varying depending on norbornene incorporation in the polymer chain.

As regards entries 3, 4, and 5 for example, it is possible to note that the $T_g$ values increase with the norbornene mol % present in the segments, as reported in Figure 2.4.

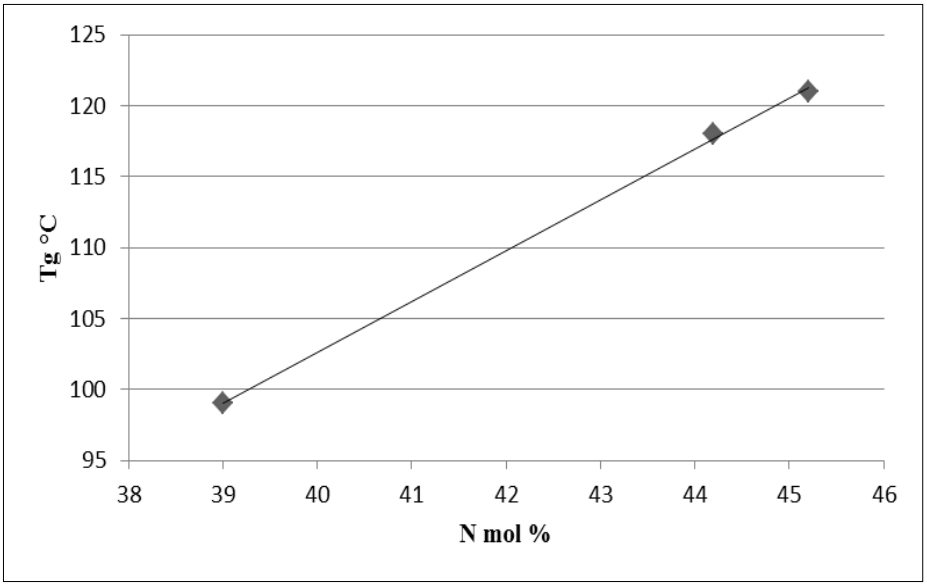


**Figure 2.4.** *Plots of norbornene content vs. $T_g$ values for entries 3, 4, and 5.*

Finally, the structure of E-*co*-N copolymers was investigated by $^{13}C$ NMR spectroscopy 4, as reported in Figure 2.5, and norbornene mol % content was calculated, as reported in Table 2.1.

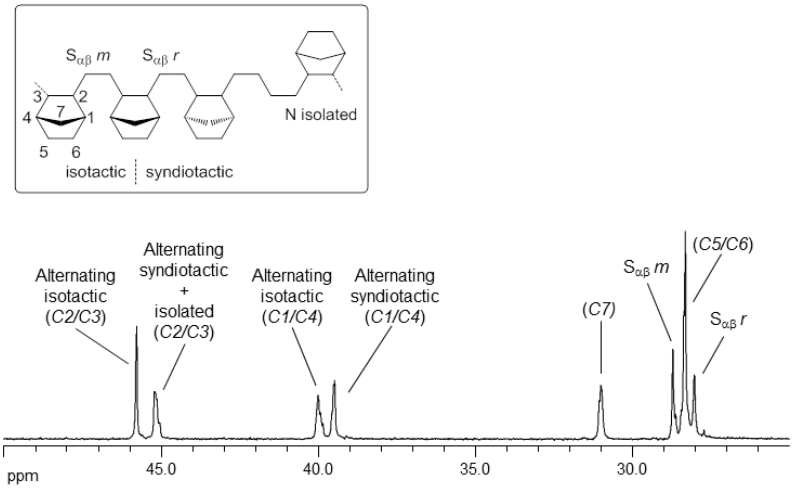


**Figure 2.5.** *$^{13}C$ NMR spectra of (a) P(E-co-N) (run 6, Table 1).*

$^{13}C$ NMR spectra of copolymers, assigned on the basis of previous investigation of the microstructure of norbornene copolymers by $^{13}C$ NMR [4] revealed alternating atactic E-*co*-N copolymers, with N enchained by *cis*-2,3-*exo* addition. An example of the $^{13}C$ NMR spectra is shown in Figure 2.5. The dominant signals are those of alternating NENE sequences and of isolated N units present in ENEE sequences. The most interesting peaks are: (i) the peaks at 45.76 ppm and at 45.20 assigned to $C_2$ and $C_3$ carbons of N in the alternating isotactic and alternating syndiotactic NENEN sequences, respectively; (ii) the signals at 28.71 and at 28.05 ppm assigned to the carbons derived from E in the alternating isotactic and syndiotactic NEN units, respectively. The signals diagnostic of ENNE sequences are absent. The relative peak intensities also revealed a quite similar content of syndiotactic and isotactic NENE sequences that indicates stereoirregularity.

## 2.3 Living block copolymers of ethylene and norbornene

The above results clearly indicate that **1**/*d*-MAO could afford the synthesis of block copolymers. Thus, PE-*block*-P(E-*co*-N) with a crystalline PE block and an amorphous atactic P(E-*co*-N) block as well as P(E-*co*-N)$_1$-*block*-P(E-*co*-N)$_2$, having different norbornene contents in the segments were synthesized. The results are reported in Table 2.2.

**Table 2.2. Conditions and results for the block copolymers synthesis by catalys 1/d-MAO**

| Run[a] | Block copolymer | $t_2$ min | $[N]/[E]_1$/ $[N]/[E]_2$ | Yield mg | $T_m$ ($\Delta H_m$)[b] °C | $T_g$ °C | N mol % | $M_n$ kg mol$^{-1}$ | $M_w$/ $M_n$ |
|---|---|---|---|---|---|---|---|---|---|
| **1**[e] | PE | - | - | 163 | 135 (167) | - | - | 111 | 1.37 |
| **14** | PE-*b*-P(E-*co*-N) | 1 | 0/2 | 266 | 134 (107) | n.o. | 7.1 (37.8)[f] | 281 | 1.20 |
| **15** | PE-*b*-P(E-*co*-N) | 2 | 0/2 | 472 | 133 (73) | 102 | 13.4 (40.7)[f] | 328 | 1.18 |
| **16** | PE-*b*-P(E-*co*-N) | 3.5 | 0/2 | 681 | 132 (51) | 100 | 18.9 (39.3)[f] | 344 | 1.18 |
| **17** | PE-*b*-P(E-*co*-N) | 5 | 0/3 | 630 | 131 (33) | 119 | 24.7 (42.9)[f] | 593 | 1.18 |
| **18** | P(E-*co*-N)$_1$-*b*-P(E-*co*-N)$_2$ | 5 | 0.5/4 | 234 | - | 53, 118 | 36.6 | 611 | 1.28 |

[a] ***1*** *= 0.5 μmol; MAO: Al/Ti = 2000/1; $V_{toluene}$ =125 mL; T = 50 °C; p(E)= 1.01 bar*
[b] *Determined by DSC, second heating scan*
[c] *Average N content determined by $^{13}C$ NMR in $C_2D_2Cl_4$ at 103 °C with HMDS as reference*
[d] *Determined by SEC in o-$C_6H_4Cl_2$ with standard PS calibration*
[e] ***1*** *= 1 μmol; MAO: Al/Ti = 2,000/1; $V_{toluene}$ = 250 mL; T = 50 °C; p(E) =1.01 bar*
[f] *Norbornene content in P(E-co-N) block.*

The former type of crystalline-amorphous block copolymer was prepared by sequential monomer addition technique. After 5 minutes homopolymerization to grow the PE block, a known amount of norbornene was added, and the copolymerization was conducted for 1, 2, and 3.5 minutes. From Table 2.2, it is possible to see that there is a progressive increase in average molecular weight with reaction time of the second block, as reported also in Figure 2.6.

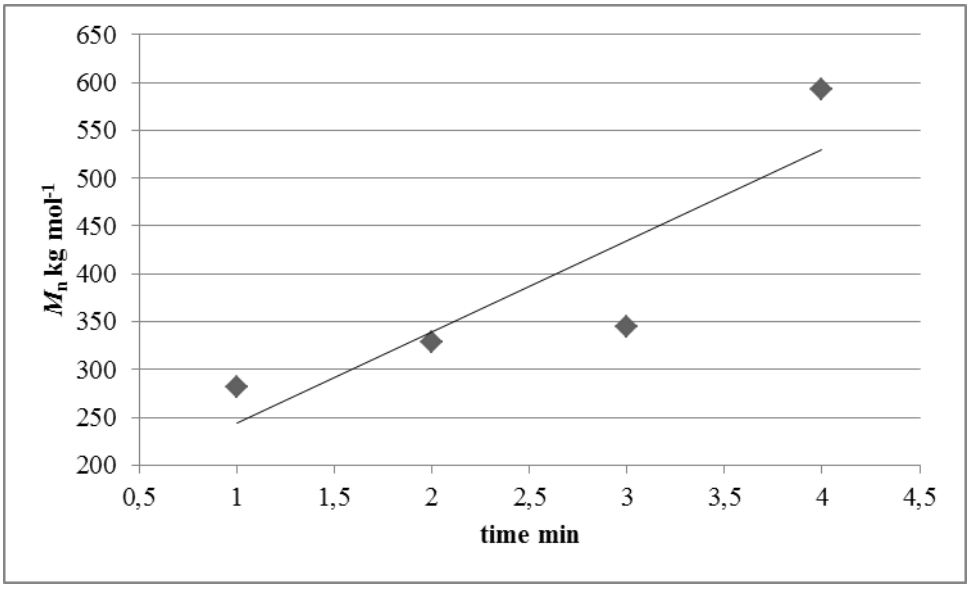


**Figure 2.6.** *Increasing of molecular weights with time for entries 14,15, 16, and 17.*

Notably, the living character is also retained in block copolymer synthesis at 50 °C ($M_w/M_n$ = 1.12-1.20).

The $^{13}$C NMR spectrum of the block copolymer (run 17, Table 2.2) is shown in Figure 2.7, and overlapping for clarity to the copolymer spectrum (run 6, Table 2.1); the resonances of the random sequences of E-*co*-N copolymer were observed together with that of PE block.

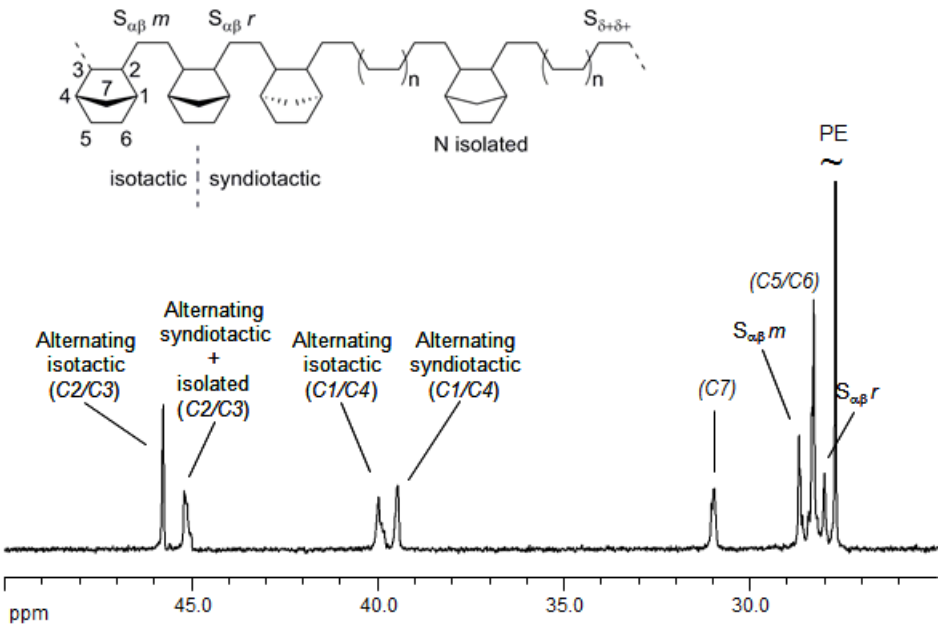


**Figure 2.7.** *$^{13}$C NMR spectra of PE-block-P(E-co-N) (run 17, Table 2.2).*

These block copolymers showed both the melting event of the crystalline PE segment and $T_g$ that corresponds to the amorphous atactic P(E-*co*-N) block (Figure 2.8).

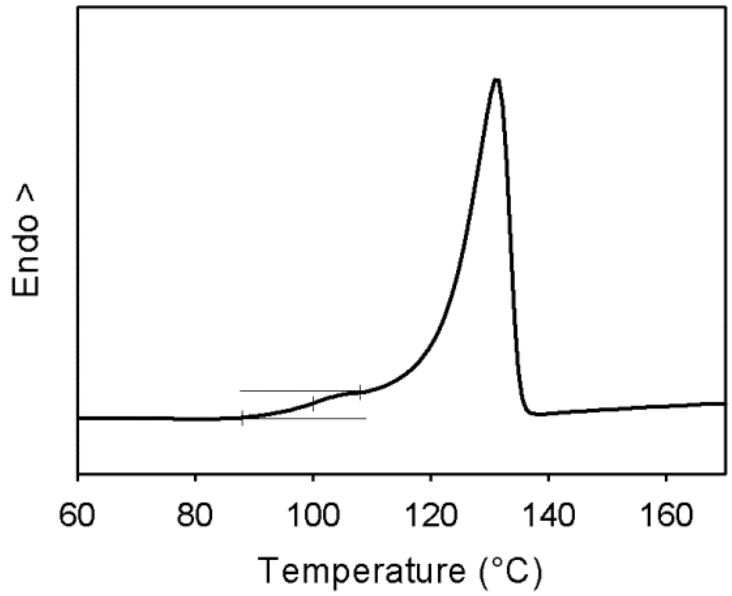


**Figure 2.8.** *Example of DSC diagrams of PE-block-P(E-co-N) (run 16, Table 2).*

The melting point of the crystalline portion of these block copolymers (PE) appears as a sharp peak. The $T_g$ values are in the range from 100 to 120 °C, as expected for corresponding P(E-*co*-N)s of Table 2.1, and thus partially overlap with the melting peak. When the amorphous block is sufficiently long, $T_g$ appears as shoulder peak. As expected, increasing the norbornene content in the second block, there is an increase in $T_g$ values and a corresponding decrease in $T_m$ values.

Interestingly, the higher the molar mass of P(E-*co*-N) block the lower the ΔH of the crystalline segment (runs 14–17, Table 2.2).

Well-defined high molar mass P(E-*co*-N)$_1$-*block*-P(E-*co*-N)$_2$ in which each copolymer segment contains a different N content was also prepared.

DSC analysis of the block copolymer clearly showed two $T_g$s related to the two blocks with different N contents (Figure 2.9).

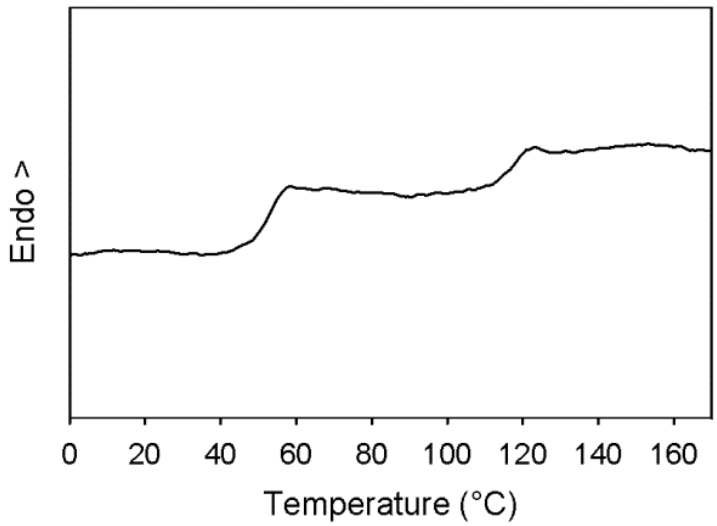


**Figure 2.9.** *DSC diagram of P(E-co-N)$_1$-block-P(E-co-N)$_2$ (run 18, Table 2.2).*

Quite different $T_g$ values, 53 and 118 °C, are obtained in line with those predictable from feed ratios employed. They are, respectively, lower and higher than the expected $T_g$ from the average norbornene content of 36.6 mol % determined by $^{13}$C NMR.

## 2.4 Conclusions

The living copolymerization of E with N with the catalytic system **1**/*d*-MAO has been investigated at temperatures between 25 and 90 °C and at different [N]/[E] feed ratios, generating very high-molar-mass and narrowly-dispersed copolymers. The living characteristics of these copolymerizations have been proven through kinetic studies at 50 °C, since this was the best temperature reaction in terms of yields, activity and molecular weights dispersity. Inspection of copolymer microstructure using $^{13}$C NMR revealed the formation of stereoirregular alternating copolymers, while thermal properties reflect norbornene content. At higher temperatures (75 and 90 °C) a slight broadening of molar masses was observed, which suggests a competition between N coordination and *o*–F interaction with the metal center, affecting the livingness to some extent.

Moreover, the excellent control over molar masses and growing of molecular weights allows for the synthesis of block copolymers based on P(E-*co*-N) and led to the generation of PE-*block*-P(E-*co*-N)s with a crystalline PE block and an amorphous atactic P(E-*co*-N) block as well as P(E-*co*-N)$_1$-*block*-P(E-*co*-N)$_2$, having different norbornene contents in the

segments. The polydispersity remains low even for the block copolymers, and the thermal properties reflect the comonomer incorporation in the chain.

## 2.4 References


1. He L.-P, Liu J.-L, Li Y.-G, Liu S.-R., Li Y.-S. *Macromolecules* **2009**, *42*, 8566; b) Long Y.-Y, Ye W.-P, Shi X.-C, Li Y.-S *J Polym Sci Part A: Polym Chem* **2009**, *47*, 6072; c) Li X.-F, Dai K, Ye W.-P, Pan L, Li Y.-S *Organometallics* **2004**, *23*, 1223; d) Ye W.-P, Zhan J, Pan L, Hu N.-H,; Li Y.-S. *Organometallics* **2008**, *27*, 3642; e) Pan L, Hong M, Liu J.-Y, Ye W.-P, Li Y.-S. *Macromolecules* **2009**, *42*, 4391; f) Ye W.-P, Shi X.-C, Li B.-X., Liu J.-Y., Li Y.-S., Cheng Y.-X., Hu N.-H. *Dalton Trans* **2010**, *39*, 9000; g) Hong M, Wang Y.-X., Mu H.-L., Li Y.-S. *Organometallics* **2011**, *30*, 4678.
2. Yu S.-M., Mecking S *J Am Chem Soc* **2008**, *130*, 13204.
3. a) Bryliakov KP, Talsi EP, Moller HM, Baier MC, Mecking S *Organometallics* **2010**, *29*, 4428; b) Moller HM, Baier MC, Mecking S, Talsi EP, Bryliakov KP *Chem Eur J* **2012**, *18*, 848.
4. a) Tritto I, Marestin C, Boggioni L, Brintzinger HH, Ferro DR *Macromolecules* **2001**, *34*, 5770; b) Tritto I, Boggioni L, Ferro DR *Coord Chem Rev* **2006**, *250*, 212.

# 3 Results and discussion 2:

## Multinuclear NMR analysis for the active species

### 3.1 Introduction

The complex [Ti($\kappa_2$-N,O-{2,6-$F_2C_6H_3N$=C(Me)C(H)C($CF_3$)O})$_2Cl_2$] upon activation with MAO has been proved to be a highly active versatile catalyst for the living synthesis of polyolefins with unprecedented molar mass control and thermal robustness [1,2,3]. Based on previous works [4,5], the origin of the living nature was attributed to the interaction of the *ortho* fluorine-aryl ligand substituents with the titanium center, thus permitting living ethylene polymerization even at temperature as high as +75 °C [6,7].

A multinuclear NMR spectroscopic analysis was performed to assess the nature of the species which take part in E-*co*-N living polymerization since to date there are no data available. The analysis involved (i) the catalytic system (**1** with MAO); (ii) the species formed after simultaneous addition of $^{13}$C-enriched ethylene and norbornene and after further addition of $^{13}$C-enriched ethylene; and (iii) species formed during norbornene homopolymerization; all the performed experiments are illustrated in Scheme 3.1.

The studies are based on $^{1}$H, $^{13}$C, and $^{19}$F NMR experiments, at different temperatures, from -10 °C up to +25 °C. In a preliminary screening, most of the studied reactions were found to be too slow in the range temperatures between -40 °C and -10 °C; therefore complete studies were performed between -10 °C and +25 °C. Analyzing signal chemical shifts, integrals and multiciplicity and by comparisons with literature data, it has been possible to completely assign the active species involved in E-*co*-N living copolymerization.

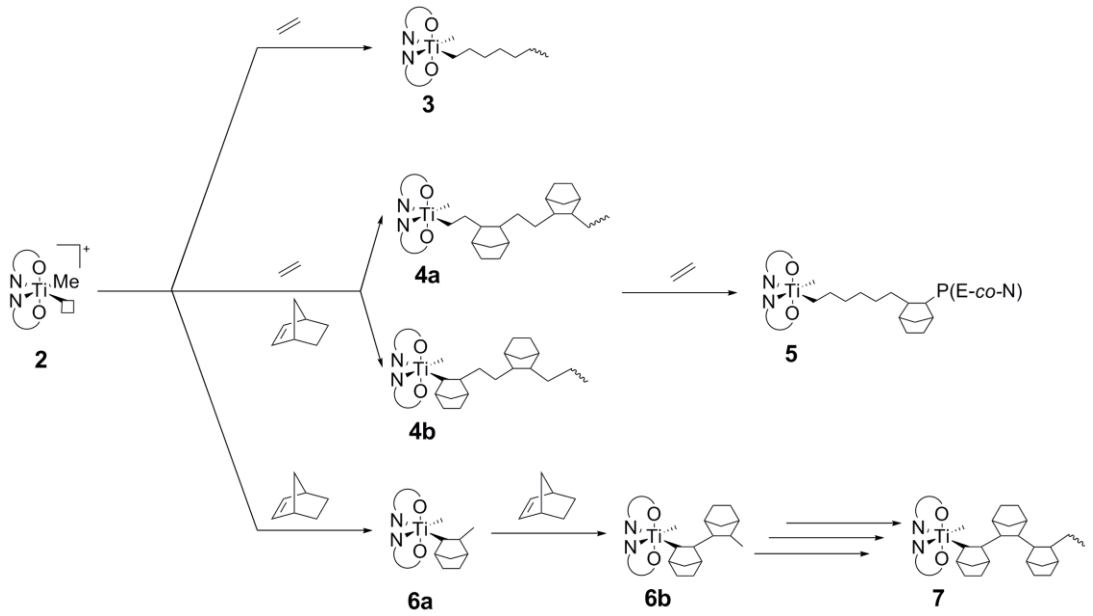


**Scheme 3.1** *Active catalytic species **2** and the resulting active species formed after additionof $^{13}$C-enriched ethylene (**3**); $^{13}$C-enriched ethylene and norbornene (**4a**, **4b**) and further $^{13}$C-enriched ethylene addition (**5**); and norbornene (**6a**, **6b**, and **7**).*

## 3.2 Active species involved in the living E-N polymerization

As a reference, NMR spectra of complex **1** with MAO were performed, in order to verify if they were comparable with literature data and to find the best instrumental operating conditions. Complex **1** was found [4] to interact with MAO to yield mainly the monomethylated species $L_2TiClMe$ at low cocatalyst loadings (Al:Ti < 40) and the ion pair $[L_2TiMe]^+$ $[MeMAO]^-$ at higher cocatalyst loadings; on this basis, the experiments were performed at Al:Ti ratios of 40, giving species **2** as reported in Scheme 3.2. After the formation of species **2**, 10 equivalents of $^{13}$C-enriched ethylene were added giving active polymeryl species **3**, in agreement with Bryliakov [5] and coworkers.

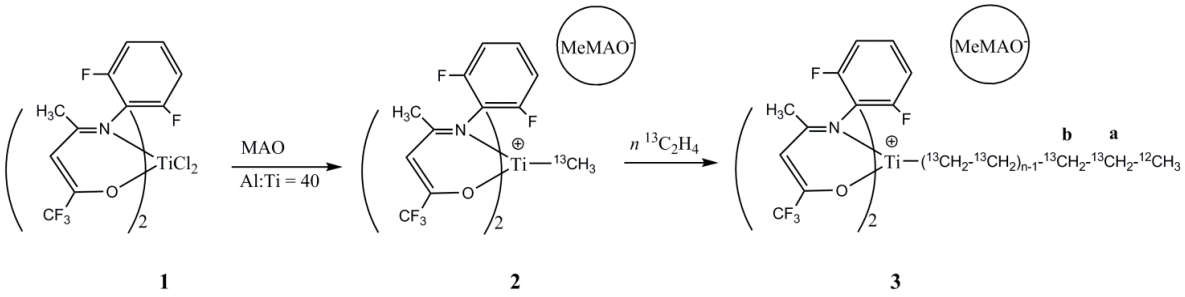


**Scheme 3.2** *Complex **1** with MAO giving ionic active species $[L_2TiMe]^+$ $[MeMAO]^-$ **2** and formation of species **3** after addition of 10 equiv $^{13}$C-enriched ethylene.*

As regard species **2**, from Figure 3.1a and Figure 3.2a, the key signals are the observed $Ti^+$-$^{12}CH_3$ resonances (δ, $^1$H: 2.8 ppm; $^{13}$C at 126.9 ppm ($J_{(CF)}$ = 8 Hz)). The $^{13}$C signal appears as a small broad triplet, since it has a very low intensity because of only 1.1 % of natural abundance of $^{13}$C in MAO. The results confirmed those by Mecking [4,5]: he reported that after the activation of the starting catalyst with $^{13}$C-MAO at -25 °C, the $^{13}$C-NMR signal of $Ti^+$-$CH_3$ relative to the cationic species was sharp and displayed a clear triplet due to the interaction of α-carbon with two *o*-fluorines ($J_{CF}$ = 7 Hz), one from each enolatoimine ligand.

Moreover, the signal deriving from vinyl proton is also detectable in the proton spectrum at 5.96 ppm. Adding $^{13}$C-enriched ethylene, it is possible to observe de appearance of a new signal related to vinyl proton at 6.08 ppm, while the former signal at 5.96 is still present, from Figure 3.1 b. This means that a new species forms, that is the so called "titanium polymeryl" one. Simultaneously, the $Ti^+$-$^{12}CH_3$ signal disappears from $^{13}$C NMR spectrum, giving rise to a new signal relative to ethylene coordination to the catalytic species metal center, that is the dublet of Ti-$^{13}CH_2$, at 145.4 ppm ($^1J$ (C,C) = 30 Hz), in Figure 3.2 b. It is also possible to identify signals related to PE peak (δ, $^1$H: 1.55-1.30 ppm; δ, $^{13}$C : 30.5 ppm), to the β carbon of the growing PE chain (δ, $^{13}$C : 28.1 ppm, Ti-$^{13}CH_2$-$^{13}CH_2$-) and to carbon named **a** (δ, $^{13}$C : 23.3 ppm, $^1J$ (C,C) = 34 Hz) and **b** (δ, $^{13}$C : 32.6 ppm) from Scheme 3.2.

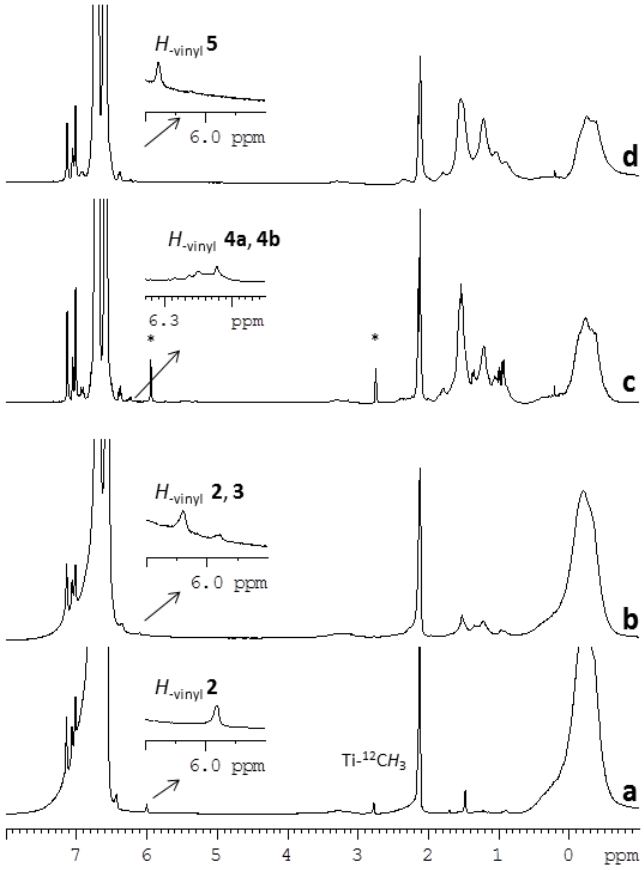


**Figure 3.1.** *$^{1}$H NMR spectra of: (a) complex **1** activated with MAO (Al/Ti = 40, [$D_8$]toluene/o-difluorobenzene, T = -10°C); (b) complex **1** activated with MAO after $^{13}$C-ethylene addition (10 equiv); (c) complex **1** activated with MAO after injection of $^{13}$C-ethylene (10 equiv) and norbornene (10 equiv); (d) sample of Figure 3.1c after additional $^{13}$C ethylene (10 equiv). Signals marked with asterisks denote free norbornene. Spectrum (a) was acquired on a Bruker 600 MHz spectrometer, while spectra (b), (c), and (d) on a Bruker 400 MHz spectrometer.*

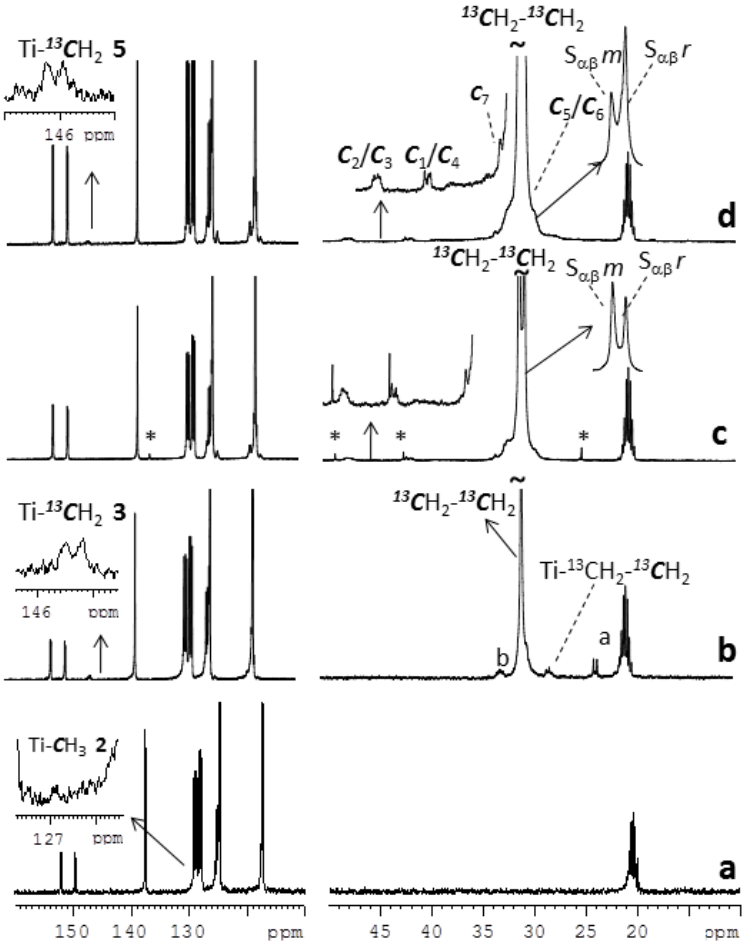


**Figure 3.2.** *$^{13}$C NMR spectra of (a) complex **1** activated with MAO (Al/Ti = 40, $d_8$ toluene/o-difluorobenzene, T = −10 °C);(b) complex **1** activated with MAO after $^{13}$C-ethylene addition (10 equiv); (c) complex **1** activated with MAO after injection of $^{13}$C-ethylene (10 equiv) and norbornene (10 equiv); (d) sample of Figure 3.2c after additional $^{13}$C-ethylene (10 equiv). Signals marked with asterisks denote free norbornene. $^{13}$C spectra were acquired on a Bruker 400 MHz spectrometer.*

Bryliakov and coworkers [8] discussed the origin of the α-C⋯*o*-F coupling, based on weak C-H⋯F-C attractive interactions, but the H,F coupling was too weak to be revealed experimentally. More realistically, they proposed an alternative explanation, involving weak non-covalent interactions between the *o*-fluorine substituents and the titanium metal center, which make it formally seven-coordinated, as illustrated in Figure 3.3.

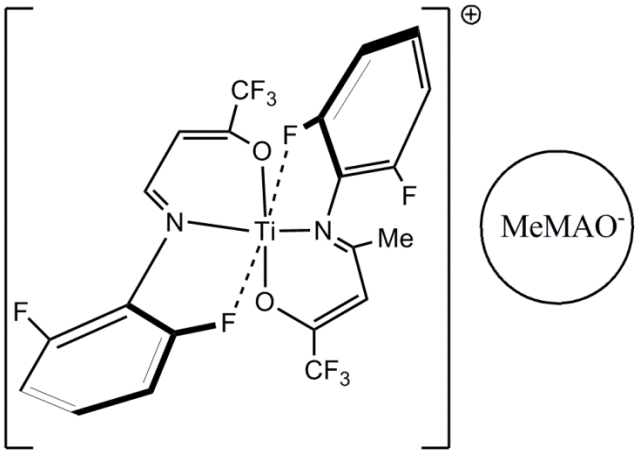


**Figure 3.3**. *The proposed o-fluorine interaction for bis(enolatoimine)titanium complex **1**.*

This interaction is expected to cause a substantial encumbrance and coordinative saturation at the metal center, which limits chain transfer to aluminum, as well as of β-H elimination or transfer to the monomer.

It is necessary also to identify the contribution of particular reactions [9,10] to the chain termination in these systems, even if β-hydride and chain transfer to the co-catalyst processes, which are reported in Scheme 3.3, should be significantly suppressed [11].

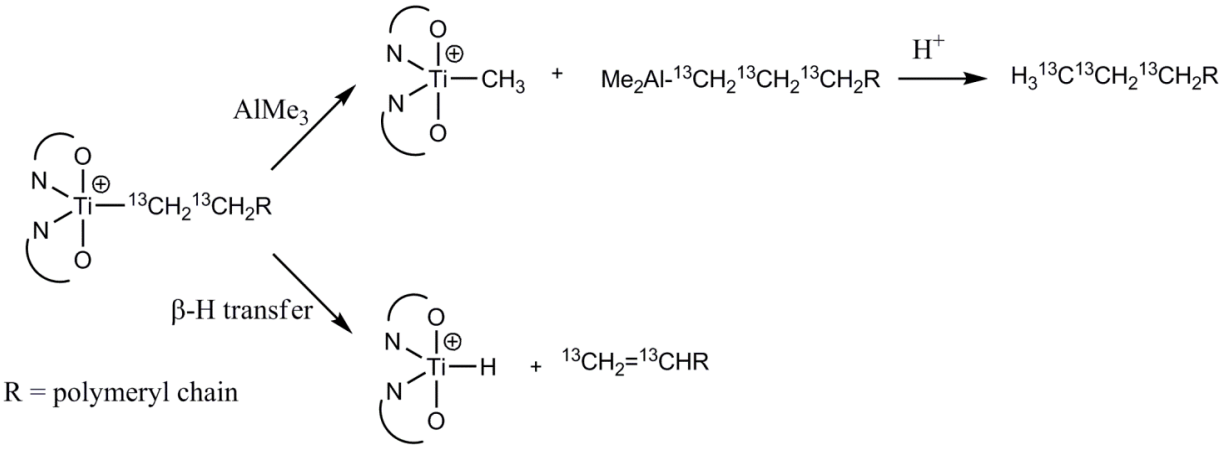


**Scheme 3.3.** *Classical chain termination mechanisms related to transfer to $AlMe_3$ or β-H transfer.*

However, a possible deactivation pathway could be the ligand transfer to $AlMe_3$, which has been found to be experimentally established for bis(salicylaldimine) and bis(enolatoimine) titanium based systems. In fact, Fujita [12] proposed a possible reaction leading to the

formation of the species $LAlMe_2$, depicted in Scheme 3.4, giving rise to a saturated-chain-ended macromolecule.

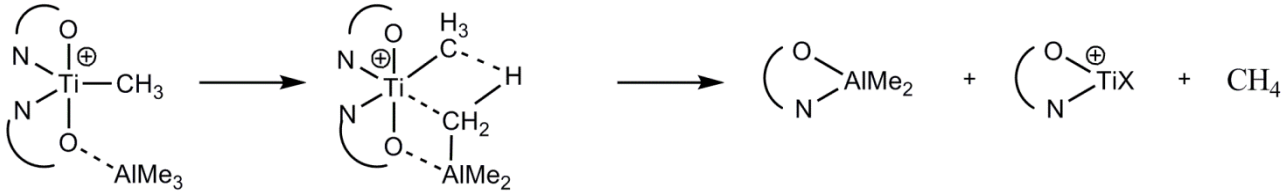

**Scheme 3.4.** *Proposed mechanism for the formation of the degradation species $LAlMe_2$*

A similar ligand transfer to $AlMe_3$ could be expected also in the course of monomer polymerization: the formation of polyethylene with saturated and unsaturated chain ends was detected, and surprisingly, the chain termination was accompanied by the insertion of a $^{12}CH_3$ terminal group, coming from $^{12}C$-methyl group of $AlMe_3$. (pathway B from Scheme 3.5, reductive elimination of $^{12}CH_3$-ended polyethylene). Nevertheless, for the catalytic system based on the analogues of complex **1** without fluorine substituents, no evidence for the formation of vinyl groups was found, which means that pathway C can operate, while $^{13}C$-NMR data of unsaturated terminal groups evidenced that they are vinylidene groups of the type $CH_2=C(CH_3)(R)$ (where R stands for polymer chain).

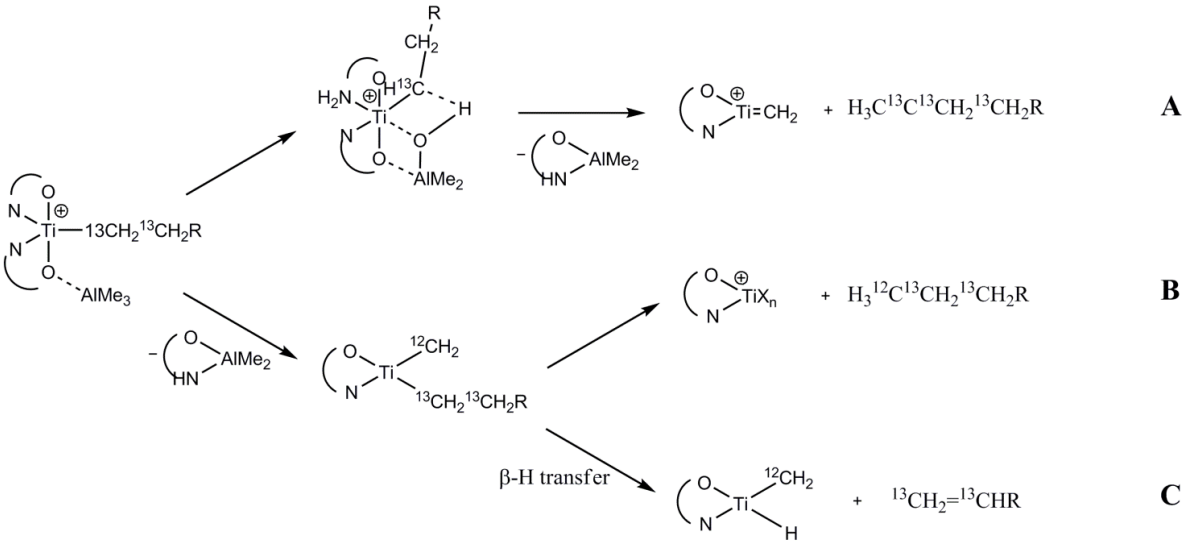

**Scheme 3.5.** *Alternative pathways associated to ligand transfer to $AlMe_3$ during polymerization.*

As regards the experiments conducted for this thesis, it is in fact possible to assign $^{13}C$ resonances of a terminal vinylidene group, that is unsaturated polymer chain ends, recorded at +25 °C ( δ, $^{13}C$: 109.4−108.8 ppm, $CH_2$=C($CH_3$)-$CH_2$-; 37.8 ppm $CH_2C(CH_3)$-$CH_2$-, which are reported in Figure 3.4. As nonlabeled MAO was used, the =C($CH_3$)- resonance, expected at 22 ppm, was not detected; the =C($CH_3$)- carbon atom expected at 145-146 ppm was not revealed due to the absence of NOE signal enhancement and because of the splitting into a doublet of doublets as the interaction with two adjacent $^{13}C$ carbon atoms.

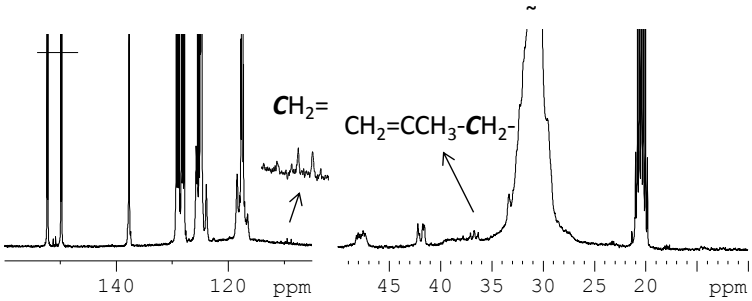


**Figure 3.4.** *Terminal vinylidene group in living ethylene polymerization with complex **1**/MAO.*

For $^{19}F$ NMR analysis of complex **1**/MAO and active catalytic species **2** with $^{13}C$ enriched ethylene addition, the results are reported in Figure 3.5a and 3.5b.

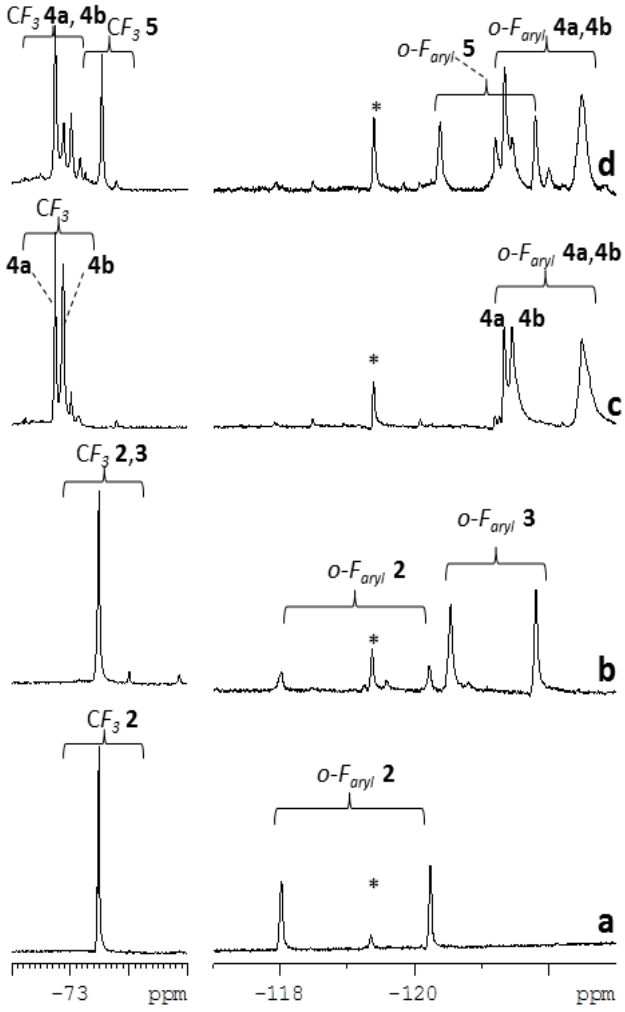


**Figure 3.5.** *$^{19}$F NMR spectra of (a) complex **1** activated with MAO (Al/Ti = 40, $d_8$ toluene/o-difluorobenzene, T = −10 °C); (b) complex **1** activated with MAO after $^{13}$C-ethylene addition (10 equiv); (c) complex **1** activated with MAO after injection of $^{13}$C-ethylene (10 equiv) and norbornene (10 equiv); (d) sample of Figure 2c after additional $^{13}$C-ethylene (10 equiv). Signals marked with asterisk denote the byproduct LAlMe$_2$. $^{19}$F spectra were acquired on a Bruker 600 MHz spectrometer.*

The results concerning the formation of species **2** and **3** are in agreement with Möller, Bryliakov and coworkers' studies [4,5]. For species **2** it is possible to identify the $CF_3$ peak at -73.5 ppm and two signals related to the *o*-fluorine substituents at -118 and -120.2 ppm. Adding ethylene, the signal of $CF_3$ moiety does not change, while it is possible to observe a shift relative to the *o*-fluorines signals at -120.5 and 121.8 ppm, due to the

influence of the inserted polyethylene chain, though still two distinct and symmetric signals are maintained.

To evaluate the reactivity of species **2** toward the copolymerization reaction, an *in situ* ethylene-*co*-norbornene polymerization was performed by adding $^{13}$C-enriched ethylene ($^{13}C_2H_4$, 10 equiv) and norbornene (10 equiv) to the solution containing species **2**. Spectra were recorded at −10 °C, since **2** was found to be stable for hours in the presence of ethylene at this temperature [2,3].

After the monomer addition, the $^{1}$H spectrum (Figure 3.1c) shows the disappearance of signals related to species **2** and the appearance of new resonances related to vinyl-H of species [TiL$_2$-E-*co*-N][MeMAO], named **4a** and **4b** in Scheme 3.1 (δ =6.2-6.3 ppm), active in the copolymerization reaction.

The $^{13}$C spectrum, in Figure 3.2c, analogously to the $^{1}$H spectrum, shows the disappearance of species **2** signals and the appearance of new resonances, assigned to alternating stereoirregular E-*co*-N copolymer according to literature data (δ, 13C: 47.8-47.1 ppm of C2/C3; 41.9-41.3 ppm of C1/C4; 33.3 ppm of C7; 30.6 ppm of C5/C6; 30.5 and 31.0 ppm of $S_{\alpha\beta}$ *r* and $S_{\alpha\beta}$ *m*) [13].

It is worth noting that the signals at 30.5 and 31.0 ppm of $S_{\alpha\beta}$ *r* and $S_{\alpha\beta}$ *m* have an integral 100 times those of the other signals due to the $^{13}$C enrichment of ethylene. Signals of Ti-$^{13}CH_2$-$^{13}CH_2$-N- and of Ti-N-$^{13}CH_2$-$^{13}CH_2$ related to species [TiL$_2$-E-*co*-N][MeMAO], named **4a** and **4b** in Scheme 3.1, active in the copolymerization reaction, are not visible. This seems to be due to the nonlabeled norbornene carbon in Ti-N- and to the presence of both *meso* and *racemic* ENEN sequences in Ti-$^{13}CH_2$-$^{13}CH_2$-N-$^{13}CH_2$-$^{13}CH_2$-N-$^{13}CH_2$-$^{13}CH_2$-. Moreover, the resonance of $^{13}CH_2$- in the isotactic ENENE sequence ($S_{\alpha\beta}$ *m*) prevails over the resonance of $^{13}CH_2$ of $S_{\alpha\beta}$ r, as in the E-*co*-N copolymer synthesized in batch. In fact, in batch copolymerization was performed at [N]/[E] = 1, T =50 °C, PE = 1 bar under continuous feed of ethylene. The copolymer produced contains 42 mol% of N. The free N here is due either to the imperfect alternating polymer or to some loss of the $^{13}C_2H_4$ ethylene during the injection by gastight syringe. Chemical shifts of nonreacted are detectable at δ = 135.5, 48.8, 42.2, and 24.9 ppm.

In the $^{19}$F experiment shown in Figure 3.5c, signals of species **2** disappear and new resonances assigned to species **4a** (*o*-F-aryl at δ = −121.3 and −122.5 ppm; CF3 at δ =

−72.7 ppm) and **4b**, (o-F-aryl at δ = −121.4 and −122.5 ppm; $CF_3$ at δ = −72.9 ppm) are visible.

The presence of two groups of signals assigned to the *o*-fluorine ligand of species **4a** and **4b** suggests that the ligand of active species in the copolymerization reaction, as observed in the living ethylene homopolymerization, retained its $C_2$ symmetry because *o*-F···Ti interactions are involved.

The *o*-F signals of **4a** and **4b** appear slightly broader than the *o*-F signals in ethylene homopolymerization. This could be related to the different microstructures of sequences of the P(E-*co*-N) copolymer chain linked to Ti. The noncovalent *o*-F···Ti interactions in species **4a**, where ethylene is the last inserted unit, play a key role in keeping the system living during the copolymerization reaction by suppressing chain termination reactions (transfer to aluminum; β-hydrogen elimination process) as in ethylene polymerization. When norbornene is the last inserted unit (species **4b**), the β-hydrogen elimination and transfer process are further disfavored because chain transfer reactions at a Ti-N bond are rather difficult. Indeed, a necessary condition for the β-hydride elimination process is the coplanarity of the Ti-C(α)-C(β)-H bond. Due to the *endo* position of the β-H atom, the typical four-center transition state cannot be formed. The second possibility, i.e., the β-hydride elimination under participation of the H atom at the bridgehead carbon atom of the norbornene, is also impossible, because of Bredt's rule.

Once the (E-*co*-N) copolymer has been formed, in order to verify the maintenance of the living character for the catalytic active species, additional $^{13}$C-enriched ethylene ($^{13}C_2H_4$,10 equiv) was added to the solution of intermediates **4a** and **4b**, and the NMR experiments were recorded at −10 °C. After the ethylene addition, resonances of nonreacted norbornene disappear in $^1$H and $^{13}$C spectra (Figure 3.1 d and 3.2d), indicating a copolymerization reaction of $^{13}$C-enriched ethylene and free norbornene, while signals of Ti-$^{13}CH_2$-$^{13}CH_2$- appear. The $^{19}$F spectrum of Figure 3.5d shows the presence of intermediate species **5** (Scheme 3.1), having a polyethylene block bonded to Ti, and reveals the simultaneous existence of species **4a** and **4b**. All these observations support the livingness of the system. By increasing the reaction temperature from −10 to 25 °C, after the monomer consumption, chain termination reactions occur (see $^{13}$C NMR spectrum in Figure 3.2). In the absence of ethylene the propagating species **5**, like species **3**, releases the polymer chain preferentially by terminal vinylidene group formation and changes. This

phenomenon is also evidenced by the $^{19}F$ spectrum (Figure 3.5d), where species **5** disappears, while species **4a** and **4b** are still present.

To gain further insight into living polymerization deriving from complex **1** activated with MAO, an *in situ* homopolymerization of norbornene was also performed. Norbornene (20 equiv) was added to species $[TiCH_3L_2][MeMAO]$, **2**, and the spectra were recorded at -10 °C. The $^{13}C$ spectrum of the reaction mixture shows the predominant resonances of nonreacted norbornene, marked with asterisks in Figure 3.6a. This indicates that norbornene homopolymerization is too slow at this temperature. By raising the temperature to +25 °C, the $^{13}C$ spectrum of Figure 3.6b evidences the decrease of free norbornene signals and the appearance of broad signals assigned to stereoirregular polynorbornene deriving from vinyl addition polymerization, with chemical shifts at δ 53.0−43.0 ppm (C2/C3); 43.0−36.0 ppm (C1/C4); 36.0−32.0 ppm (C7); 32.0−26.0 ppm (C5/C6).

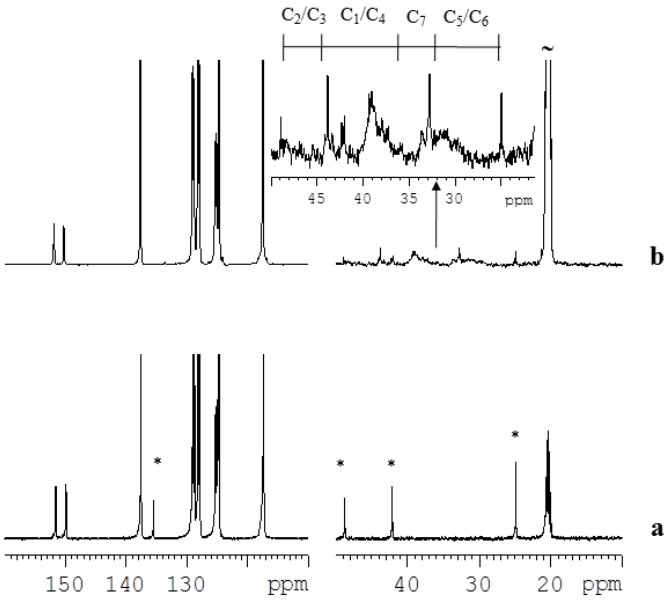


**Figure 3.6.** *a) Complex **1** with MAO with norbornene addition at -10 °C; b)Polynorbornene deriving from the sample of Figure 3.6a, increasing temperature at +25 °C.*

$^{19}$F spectrum shows the disappearance of the two signals of *o*-F of **2** and the appearance of two new groups of signals. This reveals that two active species, identified as Ti-N-$CH_3$ (**6a**) or Ti-N-N-$CH_3$ (**6b**) are formed (Scheme 3.1). Again the presence of two groups of signals indicates that the active species **6** retained the $C_2$ symmetry of the ligand, probably due to the existence of aryl *o*-F···Ti interactions, as observed in the case of PE and P(E-*co*-N) polymer reactions. Moreover, the signal multiplicity suggests that two norbornene units have been inserted and that the fluorine resonances are influenced by the microstructure of the *meso* or *racemic* NN diad bonded to titanium.

Analogously to $^{13}$C spectrum, increasing temperature to +25 °C, the fluorine spectrum in Figure 3.7 shows separated multiplets assigned to the active species **7** (Scheme 3.1). The complexity of the signals may derive from the most complex microstructure of the polynorbornene chain.

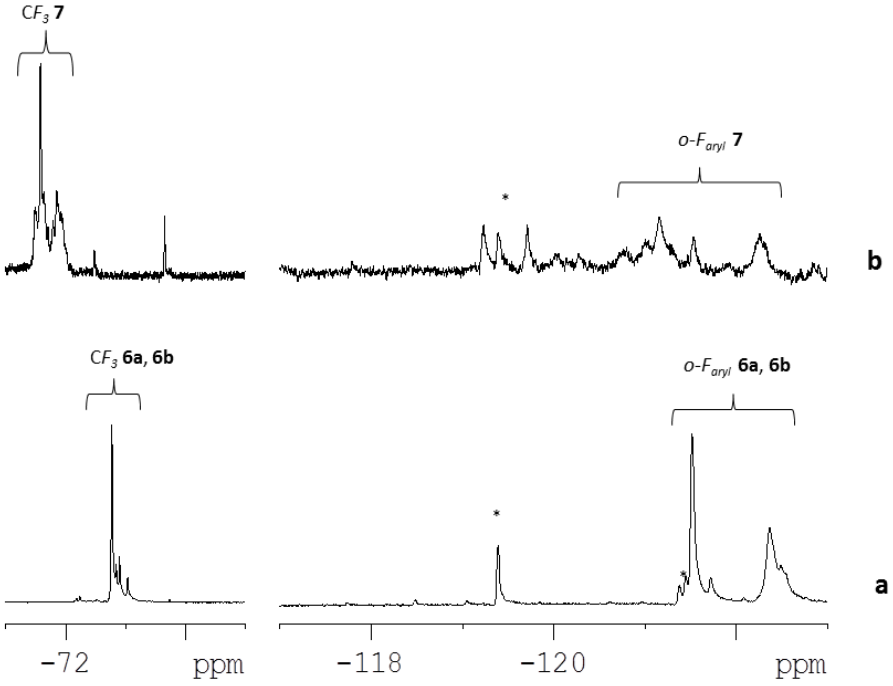


**Figure 3.7.** *a) $^{19}$F NMR spectra of complex **1** activated with MAO (Al/Ti = 40, $d_8$ toluene/o-difluorobenzene, T = −10 °C) after norbornene addition (20 equiv); (b) complex **1** deriving from sample of Figure 3.7a, T =+25 °C. Signals marked with an asterisk denote the byproduct LAlMe$_2$. $^{19}$F spectra were acquired on a Bruker 600 MHz spectrometer.*

$^{19}$F spectra are very informative; all the species have two signals (or groups of signals) for the *o*-F-aryl. The chemical shifts of *o*-F-aryl signals (Table 3.1) move toward a higher field, passing from the most to the least encumbered Ti-polymeryl or Ti-alkyl species, 7 > **6** > **4** > **5**, **3** > **2**. The difference in chemical shifts between the two signals or the two groups of signals for each species (Δδ) decreases in the following order: **7** < **6** < **4** < **5**, **3** < **2**; that is, the smaller the alkyl or polymeryl hindrance, the greater the Δδ. These data indicate that the ligand of all the Ti-polymeryl species observed retained the $C_2$ symmetry because *o*-F···Ti interactions are involved.

**Table 3.1.** ***$^{19}$F NMR assignments[a] of species deriving from complex 1 activated with MAO (Al/Ti = 40) and reacted with different monomers.***

| | ***species*** | ***CF3 ppm*** | ***o-F ppm*** | ***o-F ppm*** | ***δΔ $_{(o-F)}$ ppm*** |
|---|---|---|---|---|---|
| **$TiL_2Cl_2$ + MAO (Al/Ti = 40)** | **2** | -73.5 | -118.0 | -120.2 | 2.2 |
| **2 + $^{13}C_2H_4$ (10 equiv)** | **3** | -73.5 | -120.5 | -121.8 | 1.3 |
| **2 + ($^{13}C_2H_4$ + norbornene (10+10 equiv)** | **4a** | -72.7 | -121.3 | -122.5 | 1.2 |
| **2 + ($^{13}C_2H_4$ + norbornene (10+10 equiv)** | **4b** | -72.9 | -121.4 | -122.5 | 1.1 |
| **(4a+4b) + $^{13}C_2H_4$ (10 equiv)** | **5** | -73.5 | -120.4 | -121.8 | 1.4 |
| **2 + norbornene (20 equiv)** | **6a, 6b** | -72.8 | -121.5 | -122.4 | 0.9 |
| **2 + norbornene (20 equiv)** | **6a, 6b** | -72.9 | -121.5 | -122.5 | 1.0 |
| **2 + norbornene (20 equiv)[b]** | **7a** | -72.0 | -121.1 | -122.2 | 1.1 |
| **2 + norbornene (20 equiv)[b]** | **7b** | -72.5 | -121.5 | -122.3 | 0.8 |

[a] *$^{19}$F spectra were acquired on a Bruker 600 MHz spectrometer in d8-toluene/o-difluorobenzene, T = −10 °C.*

[b] *$^{19}$F experiments acquired at +25 °C.*

The observed highfield shift of *o*-F signals, passing from species **2** to species **7**, that is, by increasing the bulkiness of the polymer chain, suggests that the two *o*-F interactions with the titanium center are affected by the steric hindrance of the polymer chain. Indeed, the presence of two groups of signals indicates that they are still in proximity to the electron-deficient Ti center, but their highfield shift and the minor Δδ suggest that *o*-F···Ti interactions are weakened by the steric hindrance of the polymer chain. Analogously,

significant shifts are observed for $CF_3$ signals, but with an increase in the bulkiness of the growing polymer chain the signals are shifted downfield.

## 3.3 Conclusion

Multinuclear NMR studies of titanium polymeryl species formed during the norbornene copolymerization reaction with catalyst **2**, deriving from the activation of o-fluorinated bis(enolatoimine) titanium complex **1** with MAO, as well as during the in situ synthesis of PE-*block*-P(E-*co*-N) and of norbornene homopolymerization, were performed. The NMR spectroscopic studies and data from $^{19}F$ spectra, in particular, in line [3,3] with previous studies on ethylene polymerization with catalyst **2**, gave additional evidence of the importance of the *o*-F···Ti noncovalent interactions in the living character of the polymerization reaction using *o*-fluorinated bis(enolatoimine) titanium complex **1** with MAO. Indeed, as in ethylene polymerization, all the species have two signals (or groups of signals) for the *o*-F, indicating that the active species retained the $C_2$ symmetry because of *o*-F···Ti interactions. The collected NMR data indicated that by increasing the bulkiness of the polymer chain the difference between the two *o*-F decreases, and thus the *o*-F···Ti interactions become weaker. However, the *o*-F···Ti interactions also play a key role in living ethylene-*co*-norbornene polymerization, especially when ethylene is the last inserted unit; when norbornene is the last inserted unit, chain transfer reactions are already disfavored.

## 3.4 References

1. a) He L.-P, Liu J.-L, Li Y.-G, Liu S.-R., Li Y.-S. *Macromolecules* **2009**, *42*, 8566; b) Long Y.-Y, Ye W.-P, Shi X.-C, Li Y.-S *J Polym Sci Part A: Polym Chem* **2009**, *47*, 6072; c) Li X.-F, Dai K, Ye W.-P, Pan L, Li Y.-S *Organometallics* **2004**, *23*, 1223; d) Ye W.-P, Zhan J, Pan L, Hu N.-H,; Li Y.-S. *Organometallics* **2008**, *27*, 3642; e) Pan L, Hong M, Liu J.-Y, Ye W.-P, Li Y.-S. *Macromolecules* **2009**, *42*, 4391; f) Ye W.-P, Shi X.-C, Li B.-X., Liu J.-Y., Li Y.-S., Cheng Y.-X., Hu N.-H. *Dalton Trans* **2010**, *39*, 9000; g) Hong M, Wang Y.-X., Mu H.-L., Li Y.-S. *Organometallics* **2011**, *30*, 4678.
2. Ravasio A, Boggioni L, Scalcione G, Bertini F, Piovani D, Tritto I *J Polym Sci Part A: Polym Chem* **2012**, *50*, 3867.

3. Tritto I, Boggioni L, Ravasio A, Scalcione G *Macromol React Engin* **2013**, *7*, 91.
4. Bryliakov KP, Talsi EP, Moller HM, Baier MC, Mecking S *Organometallics* **2010**, *29*, 4428.
5. Moller HM, Baier MC, Mecking S, Talsi EP, Bryliakov KP *Chem Eur J* **2012**, *18*, 848.
6. Yu SM, Mecking S Jacs 2008.
7. Makio H, Fujita T *Macromol Symp* **2004**, *213*, 221.
8. Bryliakov KP, Kravtsov EA, Pennington DA, Lancaster SJ, Bochmann M, Brintzinger H, Talsi EP *Organometallics* **2005**, *24*, 5660.
9. Briliakov KP, Kravtsov EA, Pennington DA, Lancaster SJ, Bochmann M, Brintzinger H, Talsi EP *Organometallics* **2005**, *24*, 5660.
10. Talsi EP, Briliakov KP *Top Catal* **2013**, *56*, 914.
11. Britovsek GJP, Cohen SA, Gibson VC, van Meurs M *J Am Chem Soc* **2004**, 126, 10701.
12. Makio H, Oshiki T, Takai K, Fujita T *Chem Lett* **2005**, *34*, 1382.
13. (a) Provasoli A, Ferro DR, Boggioni L, Tritto I *Macromolecules* **1999**, *32*, 6697; (b) Tritto I, Marestin C, Boggioni L, Sacchi MC, Brintzinger HH, Ferro DR *Macromolecules* **2001**, *34*, 5770.

# 4 Experimental

## 4.1 General

Manipulation of air- and/or moisture sensitive materials and compounds were carried out under an inert atmosphere using a glovebox or standard Schlenk techniques. Nitrogen and ethylene were purified by passing on $CaCl_2$ and molecular sieves. Oxygen was removed by fluxing the gases through BTS catalysts. Ethylene (E) concentration in toluene was calculated according to Henry's law, as explained in paragraph 4.3.

Toluene was purchased by Fluka and distilled prior to use. Norbornene (N) was purchased by Fluka and dried before use. MAO (methylaluminoxane) was purchased by Crompton as a 10 wt % Al solution in toluene and dried in order to eliminate solvent and the free $AlMe_3$ fraction present (at 60 °C, and $10^{-2}$ atm), to obtain *d*-MAO (dried MAO).

$C_2D_2Cl_4$ was purchased from Cambridge Isotope Laboratories and used as received.

$d_8$-toluene was purchased by Cambridge Isotope Laboratories and distilled prior to use; *o*-difluorobenzene was purchased from Aldrich and distilled prior to use.

[$^{13}C_2$]Ethylene (99 % $^{13}C$) was purchased from Aldrich.

Complex [Ti($\kappa^2$-N,O-{2,6-$F_2C_6H_3N$=C(Me)C(H)=C($CF_3$)O})$_2Cl_2$] (**1**) was synthesized in the group of Prof. Mecking of Konstanz University and kindly donated 1.

## 4.2 Reagents

### 4.2.1 Toluene

The bottle of toluene was charged with $CaCl_2$, as first drying agent for few days. A proper amount of sodium/benzophenone ketyl was put in a 1 L flask equipped with a condenser, a stopcock for $N_2$/vacuum and a distillation head, and put in an oil bath. After that, toluene was transferred to the flask under $N_2$ flux. The temperature was increased up to 120 °C, and toluene was left under stirring overnight. Toluene was then freshly distilled under nitrogen atmosphere and furthermore purified with three freeze-pump-thaw cycles and finally degassed prior to use.

### 4.2.2 $d_8$-toluene

A proper amount of sodium was put under nitrogen into the flask equipped with a condenser, a stopcock for $N_2$/vacuum and a distillation head, and put in an oil bath, and $d_8$-toluene was charged. After that, benzophenone ketyl was added and the solution resulted in a blue colour. The temperature was increased up to 110 °C, toluene was left under stirring overnight.
The solvent was then distilled and finally degassed prior to use.

### 4.2.3 *o*-difluorobenzene

A proper amount of $CaH_2$ was put into the flask equipped with a condenser, a stopcock for $N_2$/vacuum and a distillation head, and put in an oil bath, and charged with *o*-difluorobenzene. After that, the temperature was increased up to 92 °C, and left under stirring overnight.
The solvent was then distilled and finally degassed prior to use.

### 4.2.4 MAO

A three necks flask was charged with the MAO solution in glovebox and then connected to a trap in liquid nitrogen. After that, the flask was putted in a oil bath at 60 °C. A $10^{-2}$ atm vacuum was applied to the trap, in order to remove the solvent. The $AlMe_3$ present inside the trap was destroyed using petroleum ether and ethanol. Finally, the white resulting dried powder was stored in the glovebox.

### 4.2.5 Norbornene

The bottle of norbornene had to be heated first, in order to have all the monomer in the liquid state. Then, a three neck 1L flask was equipped with a condenser, a stopcock for $N_2$/vacuum and a distillation head, and put in a oil bath. A proper amount of sodium was put into the flask and it was charged with liquid norbornene. The temperature was set at 80 °C, and left under stirring over sodium overnight. Finally, increasing temperature till 120 °C, norbornene was distilled in a precalibrated round bottom Schlenk ($W_1$). After having weighted again the Schlenk containing norbornene ($W_2$), some dried toluene was added, and the Schlenk ($W_3$) was weighted again. The norbornene weigh percentage content in the solution and the density of the solution was calculated as follow:

$$\%N = \frac{W_2 - W_1}{W_3 - W_1} \cdot 100$$

The density of norbornene-toluene solutions has been determined experimentally in our group. In the following table (Table 4.1) the key data obtained are reported and related graphic representation is in the following graph (Figure 4.1) .

**Table 4.1.** ***Experimental determination of density for norbornene-toluene solutions.***

| $m_{norbornene}$ g | $m_{toluene}$ g | $wt\%_{norbornene}$ % | ρ g/mL |
|---|---|---|---|
| 0 | 86.5300 | 0 | 0.86530 |
| 26.0063 | 86.8257 | 29.9523 | 0.86826 |
| 34.0531 | 86.8905 | 39.1908 | 0.86891 |
| 426919 | 86.9709 | 49.0893 | 0.86971 |
| 53.4619 | 87.1197 | 61.3660 | 0.87120 |
| 61.7396 | 87.1258 | 70.8626 | 0.87126 |
| 70.7119 | 87.3531 | 80.9495 | 0.87353 |

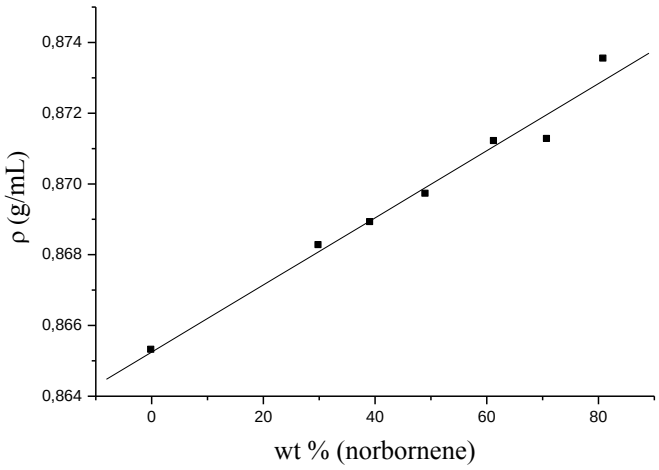


**Figure 4.1** Density of norbornene-toluene solutions

Therefore, for every norbornene-toluene solution, the density ρ is obtained from the following equation:

$$\rho = 9 \cdot 10^{-5} \cdot wt\%(N) + 0.8652$$

## 4.3 Ethylene concentration in toluene

Ethylene concentration in toluene was calculated according to Henry's law:

$$C_{Ethylene} = P_{Ethylene} H_0 e^{\frac{\Delta H_L}{RT}}$$

Where:

$C_{Ethylene}$ = ethylene concentration (M);

$P_{Ethylene}$ = ethylene pressure (atm);

$H_0$ = Henry coefficient, 0.00175 mol $L^{-1}$ $atm^{-1}$;

$\Delta H_L$ = enthalpy of solvation of ethylene in toluene, 2569 cal $mol^{-1}$;

R = universal gas constant, 1.989 cal $mol^{-1}$ $K^{-1}$;

T = temperature, K

Knowing the ethylene concentration for each experimental condition, it is possible to calculate the ratio between norbornene and ethylene in feed, and from this value, the norbornene percentage (% N) in the feed.

$$\frac{[N]}{[E]} = x \quad ; \quad [E] = \frac{1}{x} \cdot [N]$$

$$\%N = \frac{[N]}{[N]+[E]} \cdot 100 = \frac{[N]}{[N](1+\frac{1}{x})} \cdot 100 = \frac{1}{1+\frac{1}{x}} \cdot 100$$

## 4.4 Copolymerization synthesis in batch

In a glovebox, two Schlenk tubes were charged with complex **1** and *d*-MAO (Al/Ti = 2000/1) and then dissolved in toluene. A nitrogen-purged Schlenk flask equipped with a stir bar was charged with toluene by cannula. Toluene was carefully degassed by freeze-pump-thaw technique, and then saturated with ethylene at 1.1 atm. After thermal equilibration at the desired temperature (experiments were performed in a wide range of temperature, from +25 to 100 °C), the toluene solution of *d*-MAO and norbornene was added via syringes.

The polymerization reaction was initiated by adding Ti complex **1** and carried out under continuous feed of ethylene for a given time, while constantly stirring at 700 rpm.

The reaction was quenched by addition of methanol. Then, the polymer was precipitated in acidic methanol and stirred for several hours. The polymer was collected by filtration, washed with methanol, and finally dried in vacuum at 70 °C overnight.

## 4.5 Block copolymers synthesis in batch

In a glovebox, two Schlenk tubes were charged with complex **1** and *d*-MAO and then dissolved in toluene. A nitrogen-purged Schlenk flask equipped with a stir bar was charged with toluene by cannula. Toluene was carefully degassed by freeze-pump-thaw technique, and then saturated with ethylene at 1.1 atm.

After thermal equilibration at 50 °C, the toluene solution of *d*-MAO was added via syringe. The polymerization reaction was initiated by adding Ti complex **1** and carried out under continuous feed of ethylene, while constantly stirring at 700 rpm. After a predetermined time, norbornene was added via syringe, that is sequential monomer addition. The reaction was quenched by addition of methanol. Then, the polymer was precipitated in acidic methanol and stirred for several hours. The polymer was collected by filtration, washed with methanol, and finally dried in vacuum at 70 °C overnight.

A diblock P(E-*co*-N)$_1$-*block*-P(E-*co*-N)$_2$ in which each copolymer segment contains a different N content was also prepared. **1**/*d*-MAO was added to N toluene solution saturated with ethylene ([N]/[E] = 0.5) under a continuous feed of E for 5 min for the synthesis of the first poly(E-*co*-N)$_1$ segment. Subsequent addition of N (to reach ([N]/[E] = 4) to the resulting Ti-P(E-*co*-N)$_1$ formed a well-defined high-molar-mass P(E-*co*-N)$_1$-*block*-P(E-*co*-N)$_2$.

## 4.6 Copolymers Characterizations

Copolymers and block copolymers were completely characterized by $^{13}$C NMR analysis in order to obtain the fraction of norbornene incorporated in the copolymer and copolymer microstructure, by DSC and SEC analysis in order to determine $T_m$ and $T_g$ values and the molar masses, respectively.

### 4.6.1 NMR analysis for copolymers and block copolymers synthesized in batch

For $^{1}H$ and $^{13}C$ NMR about 20 mg of copolymer was dissolved in $C_2D_2Cl_4$ in a 10 mm tube. HDMS (hexamethyldisiloxane) was used as internal reference. The spectra were recorded on a Bruker NMR Advance 400 Spectrometer operating at 100.58 MHz ($^{13}C$) working in the PFT mode at 103 °C. $^{13}C$ spectra were recorded in standard 10 mm NMR tubes on a Bruker Avance 400 MHz (probe 10 mm BBI with gradient unit on Z) spectrometer operating at 9.4 T.

The acquisition parameters are: spectral width 8 kHz, 90° pulse 14.5 μs PL1 -4.00 dB, with a delay of 16 s, number of transients ~1024.

General assignments of norbornene and ethene carbons allow us to divide the spectra into four regions (50-42 ppm for $C_{2,3}$; 42-34 ppm for $C_{1,4}$; 43-30 for $C_7$; 30-25 for $C_{5,6}$ and $CH_2$ related to polyethylene) and thus to calculate the mol% of norbornene incorporated in the polymer [2].

The norbornene content, estimated as the ratio between the average intensities (I) for carbons $C_1$, $C_2$, and $C_7$ of norbornene and the total intensity for the $CH_2$ carbons (carbons $C_5$ of norbornene and E), was calculated as follows:

$$f(N) = \frac{[N]}{[N]+[E]} = \frac{\frac{1}{3}(I_{C1,4} + I_{C2,3} + 2I_{C7})}{I_{C5,6} + I_{CH_2}}$$

### 4.6.2 DSC Measurements

Differential scanning calorimetry (DSC) measurements were performed on a Pyris 1 Perkin-Elmer instrument, equipped with a liquid nitrogen device. The samples (around 8 mg) were heated from 0 to 170 °C at 20 °C/min, under a helium flow (30 mL/min). A first scan was realized to erase the thermal history of each polymer. $T_g$ were then recorded during a second thermal cycle.

### 4.6.3 SEC Measurements

Molar masses and molar masses distributions ($M_w/M_n$) were determined in *o*-dichlorobenzene at 145 °C by a GPCV2000 high temperature size exclusion chromatography (SEC) system from Waters (Millford, MA, USA) equipped with two online detectors: a viscometer (DV) and a differential refractometer (DRI). The column set

was composed of three mixed TSK-Gel GMHXL-XT columns from Tosohaas. The universal calibration was constructed from 18 narrow $M_w/M_n$ polystyrene standards, with the molar mass ranging from 162 to $5.48 \cdot 10^6$ g/mol.

### 4.6.4 NMR analysis for multinuclear NMR spectroscopic study

For the multinuclear NMR study, which was performed in order to identify the active catalytic species in the living polymerization process, $^1$H, $^{13}$C and $^{19}$F NMR experiments were performed. Spectra were acquired in a wide range of temperatures, from -40 to +25 °C, evidencing that the best results, in terms of stability of the active catalytic species, were obtained at -10 °C. Experimental uncertainties in sample temperature measurements and temperature reproducibility did not exceed ±1 °C.

$^1$H and $^{13}$C spectra were recorded in standard 5 mm NMR tubes on a Bruker Avance 400 MHz (probe 5 mm BBI with gradient unit on Z) spectrometer operating at 9.4 T and on a 600 MHz Bruker TXI (probe 5 mm with gradient unit on Z) operating at 14.1 T. $^{19}$F NMR spectra were recorded in standard 5 mm NMR tubes on a 600 MHz Bruker TXI, using the $^1$H probe detuned on $^{19}$F frequency.

Referencing is relative to the internal $CHD_2$ group of toluene at $\delta$ =2.12 ppm in $^1$H experiments, while in $^{13}$C experiments it is relative to the $CD_3$ group of toluene at $\delta$ = 20.40 ppm. $^{19}$F experiments referred to internal signals of o-difluorobenzene at $\delta$ = -139.0 ppm. Acquisition parameters for the $^1$H spectrum: 90° pulse 7.85 μs PL1-2.20 dB; number of transient 32-64; spectral width 6000 Hz. For $^{13}$C spectrum the parameters are: spectral width 32 kHz, 90° pulse 11.0 μs PL1-1.30 dB, with a delay of 10 s, on a 600 MHz spectrometer; 90° pulse 14.0 μs PL1-6.0 dB, with a delay of 10 s, on a 400 MHz spectrometer. Acquisition parameter for $^{19}$F : 90° pulse 18 μs PL1 4.0 dB, spectral width 43 kHz, number of transients 32-64.

#### 4.6.4.1 Sample preparation of complex 1

Titanium complex (0.004 mol) was weighted and placed in a 5 mm NMR tube in a glovebox. The tube was capped with a rubber septum, taken out of the glovebox, and cooled in liquid nitrogen; dry solvent (0.6 mL as 85:15 v/v $d_8$-toluene/*o*-difluorobenzene mixture) was added with a gastight syringe. After that, the sample was ultrasonicated at -10 °C for few minutes until total dissolution, cooled again in liquid nitrogen, and transferred to the probe kept at the desired temperature.

$^{19}$F NMR $d_8$-toluene/*o*-difluorobenzene, 600 MHz, T = -10 °C): δ -77.05 ppm (s, 6F, $CF_3$), -119.2 ppm (s, 2F, *o*-*F*-aryl),

### 4.6.4.2 Sample preparation for active catalytic species 2 (complex 1 + MAO)

Titanium complex (0.004 mol) and MAO (Al/Ti = 40) were weighted and placed in a 5 mm NMR tube in a glovebox. The tube was capped with a rubber septum, taken out of the glovebox, and cooled in liquid nitrogen; dry solvent (0.6 mL as 85:15 v/v $d_8$-toluene/*o*-difluorobenzene mixture) was added with a gastight syringe. After that the sample was ultrasonicated at -10 °C for few minutes until total dissolution, cooled again in liquid nitrogen, and transferred to the probe kept at the desired temperature.

$^1$H NMR ($d_8$-toluene/*o*-difluorobenzene, 600 MHz, T = -10 °C): δ 2.80 ppm (s, 3H, Ti-$CH_3$), 5.96 ppm (s, 2H, vinyl-*H*). $^{13}$C NMR ($d_8$-toluene/*o*-difluorobenzene, 400 MHz, T = -10 °C): δ 126.9 ppm (br t, Ti-$^{13}CH_3$, *J* (CF) = 8 Hz). $^{19}$F NMR $d_8$-toluene/*o*-difluorobenzene, 600 MHz, T = -10 °C): δ -73.5 ppm (s, 6F, $CF_3$), -118.0 ppm (s, 2F, *o*-*F*-aryl), -120.2 ppm (s, 2F, *o*-*F*-aryl).

### 4.6.4.3 Sample preparation for species 3 (2 + $^{13}C_2H_4$)

Titanium complex (0.004 mol) and MAO (Al/Ti = 40) were weighted and placed in a 5 mm NMR tube in a glovebox. The tube was capped with a rubber septum, taken out of the glovebox, and cooled in liquid nitrogen; dry solvent (0.6 mL as 85:15 v/v $d_8$-toluene/*o*-difluorobenzene mixture) was added with a gastight syringe. After that the sample was ultrasonicated at -10 °C for few minutes until total dissolution and cooled again in liquid nitrogen; then 10 equiv of $^{13}C_2H_4$ were added by using a gastight syringe and the sample was transferred to the probe kept at the desired temperature.

$^1$H NMR ($d_8$-toluene/*o*-difluorobenzene, 400 MHz, T = -10 °C): δ 6.08 ppm (s, 2H, vinyl-*H*), 1.55-1.30 ppm (br, -C*H*$_2$-). $^{13}$C NMR ($d_8$-toluene/*o*-difluorobenzene, 400 MHz, T = -10 °C): δ 145.4 ppm (d, Ti-$^{12}CH_2$, $^1J$ (C,C) = 30 Hz), 32.6 ppm (br t, -$^{13}C$H$_2$-$^{13}$CH$_2$-$^{12}$CH$_3$), 30.5 ppm (-$^{13}C$H$_2$-), 28.1 ppm (br t, Ti-$^{13}$CH$_2$-$^{13}C$H$_2$-, $^1J$ (C,C) = 29-30 Hz), 23.3 ppm (d, $^1J$ (C,C) = 34 Hz, -$^{13}$CH$_2$-$^{13}C$H$_2$-$^{12}$CH$_3$). $^{19}$F NMR ($d_8$-toluene/*o*-difluorobenzene, 600 MHz, T = -10 °C): δ -73.5 ppm (s, 6F, $CF_3$), -120.5 ppm (s, 2F, *o*-*F*-aryl), -121.8 ppm (s, 2F, *o*-*F*-aryl).

### 4.6.4.4 Sample preparation for species 4a and 4b (2 + $^{13}C_2H_4$ + norbornene)

Titanium complex (0.004 mol), MAO (Al/Ti = 40), and 10 equiv of solid norbornene were weighted and placed in a 5 mm NMR tube in a glovebox. The tube was capped with a rubber septum, taken out of the glovebox, and cooled in liquid nitrogen; dry solvent (0.6 mL as 85:15 v/v $d_8$-toluene/*o*-difluorobenzene mixture) was added with a gastight syringe. After that, the sample was ultrasonicated at -10 °C for few minutes until total dissolution and cooled again in liquid nitrogen; then 10 equiv of $^{13}C_2H_4$ were added by using a gastight syringe and the sample was transferred to the probe kept at the desired temperature.

$^1$H NMR ($d_8$-toluene/*o*-difluorobenzene, 400 MHz, T = -10 °C): δ 0.9-1.8 ppm (-C*H*$_2$- and norbornene-*H*), 5.94 ppm (norbornene vinyl-*H*), 6.20-6.30 ppm (br, 2H, vinyl-*H*). $^{13}$C NMR ($d_8$-toluene/*o*-difluorobenzene, 400 MHz, T = -10 °C): δ 135.5, 48.8, 42.2 and 24.9 ppm signals of carbon atoms of nonreacted norbornene; 47.8-47.1 ppm of $C_2/C_3$; 41.9-41.3 ppm of $C_1/C_4$; 33.3 ppm of $C_7$; 30.6 ppm of $C_5/C_6$; 30.5 and 31.0 ppm of $S_{ab}$ *r* and $S_{ab}$ *m* (-$^{13}$*C*H$_2$-). $^{19}$F NMR ($d_8$-toluene/*o*-difluorobenzene, 600 MHz, T = -10 °C): $\delta_{4a}$ -72.7 ppm (s, 6F, $CF_3$), -121.3 ppm (s, 2F, *o*-*F*-aryl), -122.5 ppm (s, 2F, *o*-*F*-aryl), $\delta_{4b}$ -72.9 ppm (s, 6F, CF3), -121.4 ppm (s, 2F, *o*-*F*-aryl), -122.5 ppm (s, 2F, *o*-*F*-aryl).

### 4.6.4.5 Sample preparation for species 5 (4a/4b + $^{13}C_2H_4$)

Titanium complex (0.004 mol), MAO (Al/Ti = 40), and 10 equiv of solid norbornene were weighted and placed in a 5 mm NMR tube in a glovebox. The tube was capped with a rubber septum, taken out of the glovebox, and cooled in liquid nitrogen; dry solvent (0.6 mL as 85:15 v/v $d_8$-toluene/*o*-difluorobenzene mixture) was added with a gastight syringe. After that, the sample was ultrasonicated at -10 °C for few minutes until total dissolution and cooled again in liquid nitrogen; then 10 equiv of $^{13}C_2H_4$ were added by using a gastight syringe and the sample was transferred to the probe kept at the desired temperature. After the NMR analysis, the sample was cooled again in liquid nitrogen and a further 10 equiv of $^{13}C_2H_4$ was added with a gastight syringe. The sample was retransferred to the probe precooled at the desired temperature.

$^{1}$H NMR ($d_8$-toluene/*o*-difluorobenzene, 400 MHz, T = -10 °C): δ 0.9-1.8 ppm (-C*H*$_2$- and norbornene-*H*), 6.16 ppm (s, 2H, vinyl-*H*). $^{13}$C NMR ($d_8$-toluene/*o*-difluorobenzene, 400 MHz, T = -10 °C): δ 146.1 (δ, Ti-$^{13}$*C*H$_2$, $^{1}J$ (C,C) = 30 Hz), 47.8-47.1 ppm of $C_2/C_3$; 41.9-41.3 ppm of $C_1/C_4$; 33.3 ppm of $C_7$; 30.6 ppm of $C_5/C_6$, 30.5 and 31.0 ppm of $S_{ab}$ *r* and $S_{ab}$ *m* (-$^{13}$*C*H$_2$-). $^{19}$F NMR ($d_8$-toluene/*o*-difluorobenzene, 600 MHz, T = -10 °C): δ –73.5 (s, 6F, $CF_3$), -120.4 ppm (s, 2F, *o*-*F*-aryl), -121.8 ppm (s, 2F, *o*-*F*-aryl).

### 4.6.4.6 Sample preparation for species 7 (2 + norbornene)

Titanium complex (0.004 mol), MAO (Al/Ti = 40), and 20 equiv of solid norbornene were weighted and placed in a 5 mm NMR tube in a glovebox. The tube was capped with a rubber septum, taken out of the glovebox, and cooled in liquid nitrogen; dry solvent (0.6 mL as 85:15 v/v $d_8$-toluene/*o*-difluorobenzene mixture) was added with a gastight syringe. After that, the sample was ultrasonicated at -10 °C for few minutes until total dissolution, cooled again in liquid nitrogen and transferred to the probe kept at the desired temperature.

$^{13}$C NMR ($d_8$-toluene/*o*-difluorobenzene, 600 MHz, T = + 25 °C): δ 50.0-43.0 ppm of $C_2/C_3$; 43.0-36.0 ppm of $C_1/C_4$, 36.0-32.0 ppm of $C_7$; 32.0-26.0 ppm of $C_5/C_6$. $^{19}$F NMR ($d_8$-toluene/*o*-difluorobenzene, 600 MHz, T = +25 °C): δ –71.8 to -72.5 (s, 6F, $CF_3$), -120.5 to -122.5 ppm (s, 4F, *o*-*F*-aryl).

### 4.6.4.7 Sample preparation for species 8 (3 + norbornene)

Titanium complex (0.004 mmol) and MAO (Al/Ti = 40) were weighted and placed in a 5 mm NMR tube in a glovebox and capped with a rubber septum. The tube was taken out of the glovebox and cooled in liquid nitrogen; dry solvent (0.6 mL as 85:15 v/v $d_8$-toluene/*o*-difluorobenzene mixture) was added with a gastight syringe. After that, the sample was ultrasonicated at -10 °C for few minutes until total dissolution and cooled again, then 10 equivalents of $^{13}C_2H_4$ were added by using a gastight syringe and the sample transferred to the probe kept at the desired temperature. After the NMR analysis, the sample was cooled again in liquid nitrogen and 10 equiv of solid norbornene diluted in a small amount of $d_8$-toluene were added; the sample was sonicated at -10°C for few minutes, cooled again in liquid nitrogen and transferred to the probe kept at the desired temperature.

$^{1}$H NMR ($d_8$-toluene/*o*-difluorobenzene, T = -10°C): δ = 1.14-1.98 ppm ($H_5$, $H_6$, $H_7$, and -C$H_2$- protons), δ = 2.50 ppm (s, 2H, $H_{1,4}$ *trans*), δ = 2.87 ppm (s, 2H, $H_{1,4}$ *cis*), δ = 5.33 ppm (s, 2H, $H_{2,3}$ *cis*), δ = 5.47 ppm (s, 2H, $H_{2,3}$ *trans*). $^{13}$C NMR ($d_8$-toluene/*o*-difluorobenzene, T = 0 °C): δ = 134.4 and 133.6 ppm, (*cis*-*trans* $C_2/C_3$), 45.8 - 38.0 ppm ($C_1/C_4$), 43.0 - 41.5 ppm ($C_7$), 34.0 - 32.0 ppm ($C_5/C_6$), 30.5 ppm (-$^{13}$C$H_2$-). $^{19}$F NMR ($d_8$-toluene/*o*-difluorobenzene, T = -10 °C): δ = –72.9 ppm (s, 6F, $CF_3$), δ = –121.5 ppm (s, 2F, *o*-*F*-aryl), δ = –122.6 ppm (br s, 2F, *o*-*F*-aryl).

## 4.7 References


1. Bryliakov KP, Talsi EP, Moller HM, Baier MC, Mecking S *Organometallics* **2010**, *29*, 4428.
2. Tritto I, Marestin C, Boggioni L, Zetta L, Provasoli A, Ferro DR *Macromolecules* **2000**, *33*, 8931.

# Lista dei simboli

| **Simboli** | |
|---|---|
| A | Activity |
| *a*PP | atactic popypropyleneb |
| br | broad |
| Cp | Cyclopentadienyl |
| d | doublet |
| DFT | density functional theory |
| DSC | differential scanning calorimetry |
| E | ethylene |
| GPC | gas permeation chromatography |
| *i*PP | isotactic polypropylene |
| *m* | meso |
| MAO | methylaluminoxane |
| $M_n$ | number average molecular weight |
| $M_w$ | weight average molecular weight |
| N | norbornene |
| NMR | nuclear magnetic resonance |
| PDI | polydispersity index |
| PE | polyethylene |
| P(E-*co*-N) | copolymer of ethylene with norbornene |
| PP | Polypropylene |
| PS | Polystyrene |
| *r* | racemic |
| ROMP | ring opening metathesis polymerization |
| S | Singlet |
| SEC | Size exclusion chromatography |
| t | triplet |
| TGA | thermogravimetric analysis |
| $T_m$ | melting temperature |
| $T_g$ | glass transition temperature |